EFFECTS OF IMPURITIES ON HYDRATE FORMATION

By

ANGIE PERNG SIOW YEN

FINAL PROJECT REPORT

Submitted to the Chemical Engineering Programme
in Partial Fulfillment of the Requirements
for the Degree
Bachelor of Engineering (Hons)
(Chemical Engineering)

Universiti Teknologi Petronas
Bandar Seri Iskandar
31750 Tronoh
Perak Darul Ridzuan

CERTIFICATION OF APPROVAL

EFFECTS OF IMPURITIES ON HYDRATE FORMATION

by

Angie Perng Siow Yen

A project dissertation submitted to the
Chemical Engineering Programme
Universiti Teknologi PETRONAS
in partial fulfilment of the requirement for the
Bachelor of Engineering (Hons)
(Chemical Engineering)

Approved:

Assoc. Prof. Dr. Thanabalan Murugesan
Project Supervisor

UNIVERSITI TEKNOLOGI PETRONAS
TRONOH, PERAK

June 2009

CERTIFICATION OF ORIGINALITY

This is to certify that I am responsible for the work submitted in this project, that the original work is my own except as specified in the references and acknowledgements, and that the original work contained herein have not been undertaken or done by unspecified sources or persons.

Angie

Angie Perng Siow Yen

ABSTRACT

A hydrate is a physical combination of water and other small molecules to produce a solid which has an 'ice-like' appearance but possesses a different structure than ice. The formation of hydrates can plug pipelines, equipments, instruments and restrict or interrupt the gas flow. The objectives of this research project are to study the effect of hydrogen sulfide and ethane in the equilibrium conditions of hydrate formation, effect of temperature and pressure governing the formation of the hydrate in the presence of the targeted impurities, effect of water gas ratio in feed on pressure formation of CH_4, CO_2, C_2H_6 and H_2S hydrate, effect of water gas ratio in feed on pressure formation of CH_4, CO_2, C_2H_6 and H_2S hydrate and the effect of temperature on hydrate phase equilibrium composition of CH_4, CO_2, C_2H_6 and H_2S mixture hydrate. The research project utilizes the iCON software, Excel and K-factor methods to obtain the hydrate formation temperature, pressure and phase equilibrium composition of the gas hydrate. Temperature and composition of gas and water are input as the manipulative variable whereas pressure is the dependant variable. Findings from the research show that as temperature increases, formation pressure increases. Formation pressure decreases as the amount of hydrogen sulfide and ethane content increases. Increment in water to gas ratio caused formation pressure to increase. When pressure increases, amount of impurities incorporated in the hydrate decreases.

ACKNOWLEDGEMENTS

First and foremost, the author would like to extend her greatest attitude to her supervisor, AP Dr. Thanabalan Murugesan. His endless guidance, support and encouragement have kept the author in the right track in order to finish the research project.

Besides that, the author would like to thank the Final Year Project Committee for arranging seminars to provide support and knowledge in assisting the students. The seminars are indeed very helpful and insightful. Besides that, the author would also like to thank all lecturers and technicians from Universiti Teknologi Petronas who had given her guidance throughout the period of the project.

Last but not least, not to forget the author's family members and fellow friends for all the moral support that keeps the author motivated to pursue greater heights in the project.

TABLE OF CONTENTS

LIST OF TABLES

LIST OF FIGURES

LIST OF ABBREVIATIONS

CO_2 = Carbon dioxide
CH_4 = Methane
C_2H_6 = Ethane
H_2S = Hydrogen sulfide
H_2O = Water
H = Hydrate
I = Ice
Lw = Liquid water
P = Pressure (kPa)
T = Temperature (°C)
si = mol fraction of component i, in the solid phase
V =Vapor
WGR = Water Gas ratio
yi = Mol fraction of component i, in the vapor phase

CHAPTER 1
INTRODUCTION

1.1 Background

Natural gas is a gaseous fossil fuel consisting primarily of methane and also significant quantities of ethane, propane, butane and a few non-hydrocarbon components such as hydrogen sulfide; H_2S, carbon dioxide; CO_2, nitrogen; N_2 and water.

Component	Formula	Range (mole %)
Methane	CH_4	70-90
Ethane	C_2H_6	0-20
Propane	C_3H_8	0-20
Butane	C_4H_{10}	0-20
Carbon Dioxide	CO_2	0-8
Nitrogen	N_2	0-5
Hydrogen Sulfide	H_2S	0-5
Rare gases	A, He, Ne, Xe	Trace

Table 1 Typical Composition of Natural Gases (Naturalgas.org)

Natural gas is clean burning and emits lower levels of potentially harmful byproducts into the air. Natural gas as a form of energy is used constantly to heat our homes, cook our food and generate electricity in certain parts of the world. Thus, it is the need of the energy that has elevated natural gas to such a level of importance in our society and in our lives.

The demand for natural gas has pushed the energy industries toward the discovery of remote offshore reservoirs. The ongoing development of offshore marginal oil and gas fields increases the risk of facing operational difficulties caused by the presence of gas hydrates.

According to Sloan (2000), gas hydrates or gas clathrates are crystalline compounds that formed when water forms a cage-like structure around smaller guest molecules which commonly comprises of methane, ethane, propane, isobutene, normal butane, nitrogen, carbon dioxide and hydrogen sulfide.

In the twentieth century, with the expansion of the natural gas industry, the production, processing and distribution of gas became high-pressured operations. Under pressure, it was discovered that pipelines and processing equipment were becoming plugged with what appeared to be "ice" except that the conditions were too warm for ice to form. In the 1930s, Hammerschmidt (1934) demonstrated that the "ice" was actually gas hydrates.

Research in the technologic aspects of gas hydrates is increasingly more intensive. Hydrate properties, hydrate formation and decomposition, effective means of hydrate control in systems of natural gas extraction, transport and processing, and new technologies based on the properties of hydrates.

1.2 Problem Statement

Discovered in the 1778, the gas hydrates was not of industrial interest until these hydrates where found to be causing much problems in the oil and gas industry at late 1930s. The formation of the hydrate plugs can cause two types of failures at a pipeline restriction (orifice), obstruction (flange or valve), or a sharp change in direction (bend, elbow or tee). First, hydrate impact can fracture a pipe, and second, extreme gas compression can cause pipe rupture downstream of the hydrate path.

Examples of the danger of the gas hydrate can be proven by accidents that happened at major oil and gas plants throughout the world.

i. **1970's-Elf Aquitaine North Sea Incident**

ii. **Mid 1980's-Statoil North Sea Incident**

iii. **1991-Chevron accident**

   The sour-gas flowline failed when a foreman and an operator was trying to remove the hydrate mass resulting in the death of the foreman.

iv. **1991-Gulf Oil Incident**

   Hydrate plug at formed in the overhead line from the amine contractor. The line had been depressured to the flare system, downstream to the plug. Unnoticed rapid temperature rise causes the overhead line to come apart, killing the chief operator. Loss amount to US 6 million.

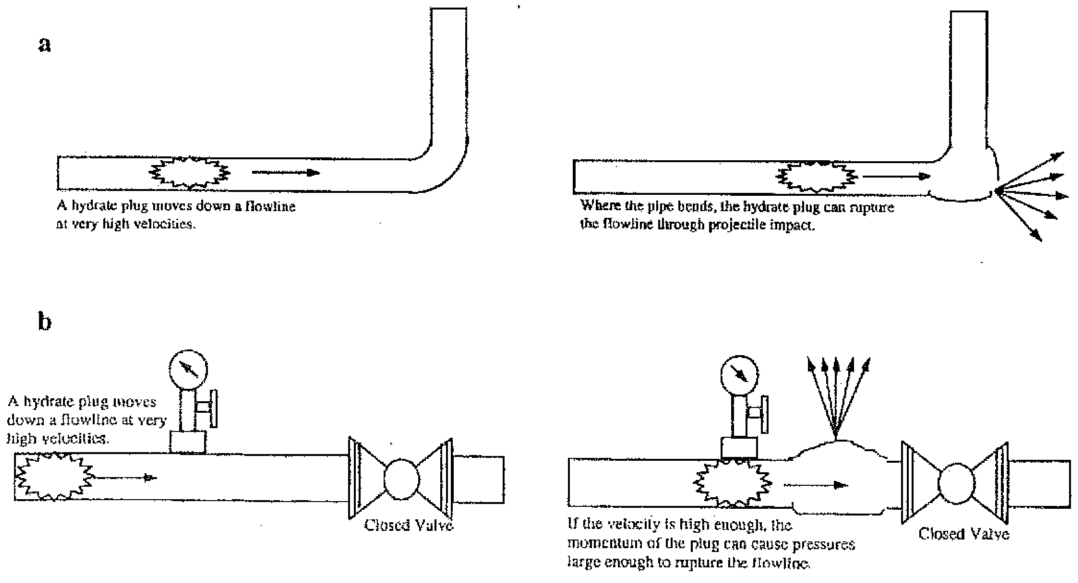

Figure 1 Hazard for moving plugs (Sloan, 2000)

1.3 Objectives

The objectives of this research are:

1. To study the effect of hydrogen sulfide, H_2S and ethane, C_2H_6 on gas hydrate formation.
2. To study the effect of temperature on pressure formation of hydrate in the presence of the targeted impurities
3. To study the effect of water gas ratio in feed on pressure formation of CH_4, CO_2, H_2S hydrate and CH_4, CO_2, C_2H_6, H_2S hydrate.
4. To study the effect of temperature on hydrate phase equilibrium composition of CH_4, CO_2, H_2S and CH_4, CO_2, C_2H_6 , H_2S mixture hydrate.

1.4 Scope of Study

The research project utilized the iCON software to predict the behaviors of the gas hydrate. The study focused on gathering thermodynamic data of hydrogen sulfide, ethane and methane hydrates, manipulation of operating parameters such as temperature and pressure of the feed stream. Different composition of natural gas and water gas ratio is also used. Besides that, K-Chart Method is used to obtain the hydrate phase equilibrium composition of the mixture hydrate.

1.5 Relevancy of the Project

Gas hydrates is of interest due to three primary reasons:

i. Production (flow assurance) problems

Gas hydrates spontaneously form in petroleum production equipment and pipelines associated with deep-water petroleum production and arctic on-shore petroleum production. These unwanted hydrates can clog equipment, preventing the optimum production of hydrocarbons.

ii. Gas hydrates are a potential energy resource

Considering the planet as a whole, the quantity of natural gas in sedimentary gas hydrates greatly exceeds the conventional natural gas resources (for example, Kvenvolden, 1993). As a result, numerous studies have discussed the energy resource potential of gas hydrates (for example, Collett, 1993, 1997, 2002; Iseux, 1992; Kvenvolden, 1993; Milkov and Sassen, 2003).

However, utilization of gas hydrates as an energy resource has been largely inhibited by the lack of economical methods for production for most hydrate accumulations. A variety of different mechanisms have been proposed for economically developing gas hydrates as an unconventional gas source.

iii. The role of gas hydrates in past and future climate changes

According to Oil Tracers (2007), gas hydrates are also of interest because of their potential role in climate change. Gas hydrates in continental shelf sediments can become unstable either as a result of warming bottom water, or as a result of a pressure drop due to a reduction in sea level. If these marine gas hydrates begin to rapidly disassociate into gas + water, then the methane trapped in the gas hydrates can be released to the atmosphere.

Methane is a greenhouse gas, methane is many times more effective as a greenhouse gas than is CO_2. According to Oil Tracers 2007, if the flux of methane to the atmosphere from dissociating hydrates is sufficient in quantity, this methane can cause global warming. This process is believed to have influenced past climate changes (for example, Henriet, 1998; Haq, 1998; Hesselbo et al., 2000; Kvenvolden, 1991), and may enhance the current global warming episode by way of a "positive feedback" loop. Specifically, as the earth warms, increasing bottom water temperatures could cause gas hydrate disassociation in many marine shelf locations. This gas hydrate disassociation would cause further warming due to the greenhouse effects of the gas which is released.

1.6 Feasibility of project within scope and time frame

Final year project is a course which is conducted for two semesters. In the first semester, the project covered on the literature reviews for gas hydrate formation and also familiarization with the iCON software. The second semester focused on the simulation by the iCON software and comparison with the manually calculated K-Factor method.

CHAPTER 2

LITERATURE REVIEW

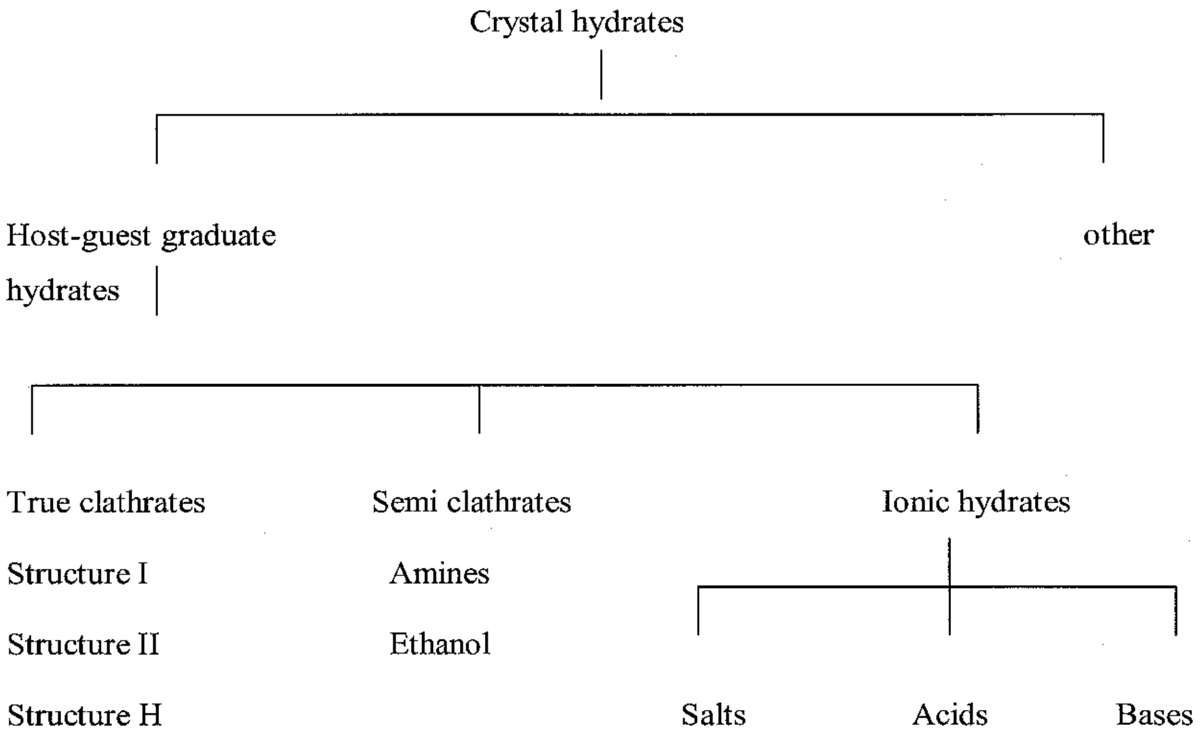

Figure 2 : Schematic representation of hydrate types (Makagon, 1997)

Gas hydrates is a mineral of the clathrate hydrate group widely spread in nature. Generally there are three types of structure for hydrates. Structure I (SI) is a body centered cubic structure which contains 46 water molecules and small natural gas molecules. Structure II (S II) is a diamond lattice within a cubic framework and contains 136 water molecules. This structure forms when natural gases or oils contains molecules larger than ethane but smaller than pentane. S II commonly occurs in hydrocarbon production and processing conditions. Structure H (SH) is named for its hexagonal framework and has large cavities enough to contain molecules the size of common components like naphtha and gasoline.

The water molecules referred to as the host molecules, and the other compounds (for example ethane, propane), which stabilize the crystals, are called the guest molecules. Carroll, 2003 states that the stabilization resulting from the guest molecule is postulated to be caused by van Der Waals forces. No bonding occurs between the host and guest molecules as the guest molecules are free to rotate in the cages built up from the host molecules.

The most encountered hydrates have the cubic Structure I and II. Their lattices are the least different energetically from the ice lattice, and the molar ratio of water and hydrate former varies between 5.75 and 17.

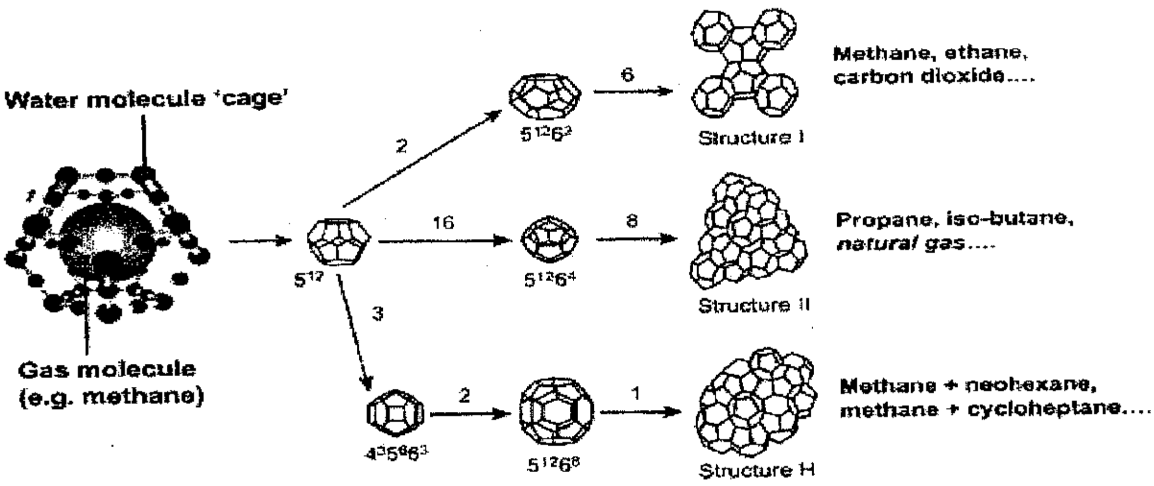

Figure 3 :Type of gas structure (Gas Hydrate Research, 2007)

Equilibrium curves for common hydrate formers at temperatures below 0°C can be seen from Figure 4 below. Equilibrium content of water vapor above hydrate is significantly lower than above liquid water or ice.

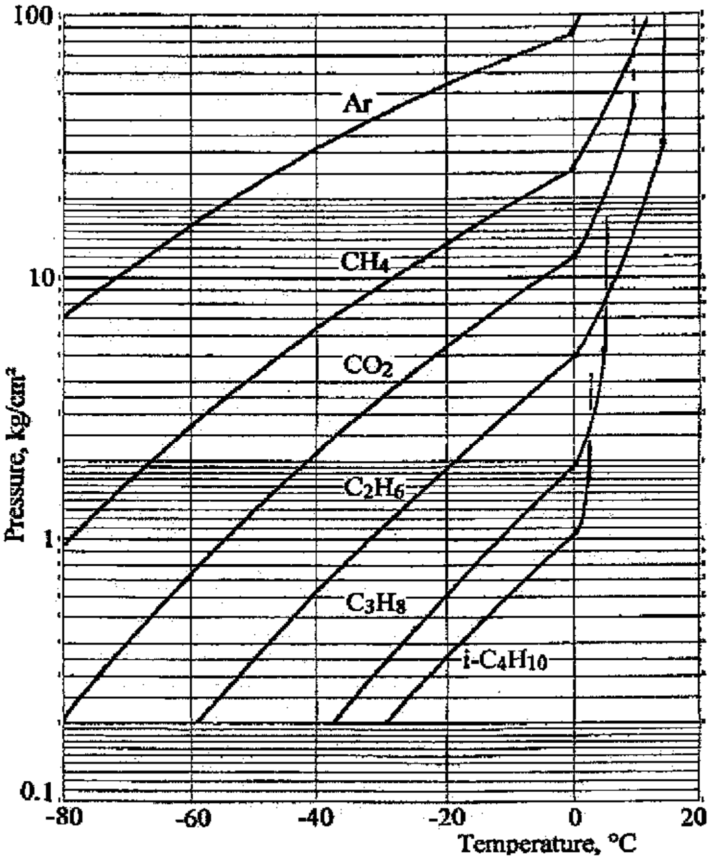

Figure 4 Hydrate formation with different gases at T<0°C (Makagon, 1997)

2.1 Brief History of Gas Hydrates

In the early 1820's, Davy and Faraday discovered hydrates while working in Davy's lab in the. They reported the dissociation of an ice-like solid that formed above the freezing point of water in mixtures of chlorine and water. Since then, many researchers have attempted to identify the hydrate forming components as well as he pressure and temperature conditions for hydrate dissociation.

When Hammerschmidt (1934) determined hydrates in pipelines, he published a correlation summary of over one hundred hydrate formation data points. Shortly afterwards, Professor D.L. Katz and his students at the University of Michigan began an experimental study, and came out with two correlative methods, one of which is the *gas gravity* method.

Wilson, Carson and Katz (1941) then came out with a initial predictive method called K_i method for hydrates on a water-free basis. Establishment of the K_i value (defined as the component mole fraction of ratio in the gas to the hydrate phase) for each of the number of components enabled the user to determine the pressure and temperature of hydrate formation from the mixtures.

2.2 Conditions for hydrate formation

Hydrate formation is a time dependent process. Gas composition, presence of crystal nucleation sites in the liquid phase, degree of agitation, temperature and pressure all contributes to the formation of gas hydrates. During the transient 'hydrate formation period' the liquid water present is termed 'metastable liquid'. Metastable water is liquid water at which in equilibrium will exist as hydrate.

According to Carroll 2003, the formation of a hydrate requires three conditions:

i. ***The right combination of temperature and pressure.***

Hydrate formation is favored by low temperature and pressure. The exact temperature and pressure depends on the composition of the gas; however hydrates form at temperature greater than 0°C (32°F).

ii. ***A hydrate former***

Type I hydrate formers include methane, ethane, carbon dioxide and hydrogen sulfide. In the hydrates of methane, carbon dioxide and hydrogen sulfide, the guest molecules can occupy both small and large cages. On the other hand, the ethane molecule occupies only the large cages.

iii. ***Sufficient amount of water***

The molar ratio of water and hydrate former for Type I and II hydrates varies between 5.75 and 17.

Typically, hydrate formers cannot be removed from the mixture. Thus, only condition **i** and **iii** can addressed to prevent hydrate formation.

Other phenomena that can enhance hydrate formation include:

i. ***Turbulence***

High velocity: Hydrate formation is favored in regions where the fluid velocity is high. This makes choke valves particularly susceptible to hydrate formation. First, there is usually a significant temperature drop when natural gas is choked through a valve because of the Joule-Thomson effect. Secondly, the velocity is high through the narrowing in the valve.

Agitation: Mixing in a pipeline, process vessel, heat exchangers enhance hydrate formation.

ii. ***Nucleation sites***

Nucleation sites for hydrate formation include an imperfection in the pipeline, a weld spot, a pipeline fitting (example; elbow, tee, valve). Silt, scale, dirt and sand make good nucleation sites as well.

iii. ***Free water***

Free-water is not necessary for hydrate formation, but the presence of free-water enhances hydrate formation. In addition, water-gas interface is a good nucleation site for hydrate formation.

2.3 Thermodynamic hydrate prevention methods

According to Sloan, 2000, hydrate can be prevented by these thermodynamic prevention methods.

1. Reducing the water concentration from the system. Unfortunately, water removal is not feasible between the wellhead and the platform.
2. Operating at temperatures above the hydrate formation temperature for a given pressure by insulation the pipelines or applying heat. High reservoir fluid temperature may be retained through insulation and pipe bundling, or heat may be added through hot fluids or electrical heating, but this option is not very economical.

iii. Operating at pressures below the hydrate formation pressure for a fixed temperature. This in turn lowers the density, and leads to declining of pipeline transportation efficiency.

iv. Adding inhibitors such as salts, methanol, and glycols to inhibit the hydrate formation conditions and shift equilibrium curve to a higher pressure and lower temperature.

2.4 Hydrate Nucleation

Hydrate nucleation is a process, during which small hydrate crystals (nuclei) grow and disperse in an attempt to achieve critical size for continued growth. While the nucleation step is a microscopic phenomenon involving tens to thousands of molecules which is difficult to be observed experimentally (Mullin, 1993). Current hypothesis for hydrate nucleation are based upon the better known phenomena of water freezing, the dissolution of hydrocarbon in water, and computer simulations of both phenomena.

2.5 Mechanism of hydrate formation

As a result of experimental studies it was determined (Makagon, 1997) that the process of hydrate formation starts at the free gas-water surface:

a) on a free contact surface of liquid water-gas or liquid water-liquid gas
b) on the surface of the water drop-water film that condensed in a gas volume
c) on the surface of gas bubbles that separate out within a water volume
d) on the interface of the condensed gas drops-dispersed condensed gas, as the condensed gas evaporates within a volume of free gas saturated with water vapors
e) on the water-metal interface where the adsorption of the molecules of gas dissolved in the water takes place.

2.6 Equations of State

Fanchi and John R.(1997) states that an equation of state is a formula describing the interconnection between various macroscopically measurable properties of a system. For physical states of matter, this equation usually relates the pressure, temperature, volume, and number of atoms to one another.

There are two types of equation of states namely virial and cubic equations. However, commercial reservoir simulations generally employ the cubic ones (Smith, J.M et al., 2005). Polynomial equations that are in molar volume offer a compromise between generality and simplicity that is suitable to many purposes. According to Danesh and Ali (1998), cubic equations are in fact the simplest equations capable of representing both liquid and vapor behavior.

Reservoir simulation software normally provides several equations of states as the calculation basis to choose from. Various equations of states need to be available to cover different reservoir characters. The common equations of states need to be available vary from Peng-Robinson, Redlich-Kwong, and Zudkevitch-Joffe-Redlich-Kwong.

Van der Waals equation which is commonly referenced in textbooks and papers for historical reasons, it is now almost obsolete. Other slightly complex equations are much more accurate. Gases are treated either as ideal gas or real gas. Although no gas is truly ideal, many gases follow the ideal gas low very closely at sufficiently low pressures. Ideal gas law which was determined empirically is:

$$\boxed{PV = nRT} \tag{2-1}$$

P = pressure

V = volume

n = moles of substances

R = ideal gas constant

T = temperature

Elliot et al.(1999) states ideal gas law is valid with assumptions that the molecules or atoms of the gas are monoatomic, possessing mass but no significant volume, and undergo only elastic collisions with each other and the sides of the container in which both linear momentum and kinetic energy are conserved.

However, these assumptions are not always fulfilled in reality. Thus, these equations are modified to comply with the characteristics of real gases. Real gas laws try to predict the true behavior of a gas better than the ideal gas law by putting in terms to describe attractions and repulsions between molecules.

2.6.1 Van der Waals equations of states

In 1873, while searching for a way to link the behavior of liquids and gases, Dutch physicist Johannes van der Waals developed an explanation for these deviations and an equation that was able to fit the behavior of real gases over a much wider range of pressures.

As the volume of real gas is too large at high pressures, van der Waals introduced a constant *b* into the ideal gas equation that was equal to the volume actually occupied by a mole of gas particles. A term from the volume of real gas is subtracted before being substituted into the ideal gas equation. Volume of the gas particles depends on the number of moles of gas in the container, thus the term that is subtracted from the real volume of the gas is equal to the number of moles of gas (n) times b.

$$\boxed{P(V-nb) = RT} \qquad (2\text{-}2)$$

The term nb is insignificant when the pressure is relatively small and the volume is reasonably large. Another assumption is that there is no force of attraction between gas particles. In reality, small forces of attraction between gas molecules exist.

To correct the incorrect assumptions that pressure of real gas is smaller than expected from the ideal gas equation, van der Waals added a term of pressure into the equation.

Therefore, the complete van der Waals equation is as follows:

$$\boxed{\left(P+\frac{a^2}{V_m^{\ 2}}\right)(V_m-b)=RT} \qquad (2\text{-}3)$$

Where a and b can be determined either empirically for each individual compound or estimated from the relations:

$$\boxed{a=\frac{27R^2T_c^{\ 2}}{64P_c}} \quad \text{and} \quad \boxed{b=\frac{RT_c}{8P_c}} \qquad (2\text{-}4),\ (2\text{-}5)$$

T_c = critical temperature

P_c = critical pressure

2.6.2 Redlich-Kwong equation of states

Redlich-Kwong equation of states is of interest primarily due to its relatively simple form. While superior to the van der Waals equations if states, it performs poorly with respect to liquid phase and thus cannot be used accurately to calculate vapor-liquid equilibrium.

The Redlich-Kwong equations of states is adequate for calculation of gas phase properties when the ratio of the pressure to the critical pressure is less than one-half of the ratio of the temperature to the critical temperature:

$$\boxed{\frac{P}{P_c}<\frac{T}{2T_c}} \qquad (2.6)$$

The Redlich-Kwong equation is:

$$\boxed{\left(P+\frac{a}{V_m(V_m+b)T^{\frac{1}{2}}}\right)(V_m-b)=RT} \qquad (2.7)$$

with $\boxed{a=\frac{27R^2T_c^{\,2}}{64P_c}}$ and $\boxed{b=\frac{RT_c}{8P_c}}$ (2.8), (2.9)

P = pressure

T = temperature

V_m = molar volume

R = ideal gas constant

b = empirical constant

2.6.3 Soave-Redlich Kwong equation of states

Soave replaced the term $aT^{-0.5}$ of the Redlich-Kwong equation with a function $\alpha(T,\omega)$ involving temperature and accentric factor. The α function was devised to fit the vapor pressure data of hydrocarbons. Soave-Redlich-Kwong equation of states is quite capable of predicting vapor-liquid equilibrium, but does not provide reliable liquid density according to Danesh, Ali (1998).

$$\boxed{\left(P+\frac{a}{V_m(V_m+b)}\right)(V_m-b)=RT} \qquad (2.10)$$

where $\boxed{\alpha=(1+(0.480+1.574\omega-0.176\omega^2)(1-T_r^{\,0.5}))^2}$ (2.11)

with $\boxed{a=\frac{0.42747R^2T_c^{\,2}}{P_c}}$ and $\boxed{b=0.08664\frac{RT_c}{P_c}}$ (2.12), (2.13)

2.6.4 Peng-Robinson equation of states

Peng-Robinson modified the attractive term to improve the prediction of equations of liquid density in comparison with Soave-Redlich-Kwong equation of states. This equation is given by:

$$\boxed{\left(P+\frac{\alpha a}{V_m(V_m+b)+b(V_m-b)}\right)(V_m-b)=RT} \qquad (2.14)$$

where $\boxed{\alpha=(1+(0.480+1.574\omega-0.176\omega^2)(1-T_r^{0.5}))^{0.2}}$ (2.15)

with $\boxed{a=\frac{0.457235R^2T_c^{\,2}}{P_c}}$ and $\boxed{b=0.077796\frac{RT_c}{P_c}}$ (2.16), (2.17)

Both Soave-Redlich-Kwong and Peng-Robinson are possible candidate for the calculation of hydrate phase equilibrium as long as solid phase does not play a significant role.

2.7 Hydrate calculation method

The initial problem surfaced when designing processes involving hydrates are to predict the formation temperature ands pressure. There are a series of method that can be used to predict the formation conditions either by manual calculation or computer programs.

Manual calculation methods are useful for estimation of hydrate formation condition. Unfortunately, the drawback of these methods is that they are not highly accurate. However, these methods remain quite popular.

Two methods commonly applied tribute to Katz and co-workers are “gas gravity” and the “K-factor” method.

2.7.1 Gas Gravity Method

The gas gravity method was developed by Professor Katz and co-workers in the 1940s. This method involves a single chart which relates pressure, temperature and specific gravity of the gas. Given the molar mass of the gas, M, the gas gravity, γ can be calculated as follows:

$$\boxed{\gamma = \frac{M}{28.966}} \tag{2.18}$$

The value 28.966 is the standard molar mass of air.

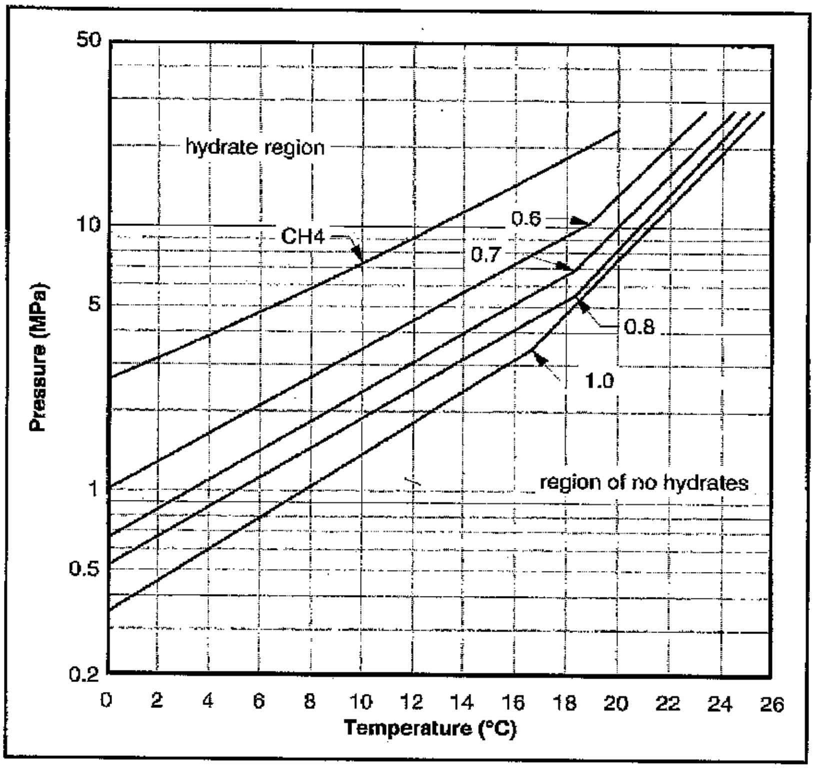

Figure 5 Hydrate locus for sweet natural gas using gas gravity method (Carroll, 2003)

From Figure 5, if the value calculated is to the left and above the appropriate gravity curve, then hydrate will form. This chart, however an approximation is and should only be used as such.

2.7.2 K-Factor method

Originated from Carson and Katz (1942), this method is defined as the distribution of the component between the hydrate and the gas:

$$\boxed{K_i = \frac{y_i}{s_i}} \tag{2.19}$$

Where y_i and s_i are the mole fractions of component i in the vapor and hydrate respectively. These mole fractions are ona free-water basis, and water is not included in the calculations. It is assumed that sufficient water is present to form a hydrate.

The evaluation for K value for CH_4, CO_2, C_2H_6 and H_2S can be done using the proposed formula by Sloan, 1997 as:

$$\begin{aligned}\ln K = {} & A + B*T + C*\pi + D*T^{-1} + E*\pi^{-1} + F*T*\pi + G*T^{2} + H*\pi^{2} + \\ & I*\pi*T^{-1} + J*\ln(\pi*T^{-1}) + K*(\pi^{-2}) + L*T*\pi^{-1} + M*T^{2*}\pi^{-1} + N*\pi*T^{-2} + \\ & O*T*\pi^{-3} + P*T^{3} + Q*\pi^{3}T^{-2} + R*T^{4}\end{aligned} \tag{2.20}$$

where π = pressure in psia, T = temperature, °F

The K-value charts were generated for methane, ethane, propane, carbon dioxide, hydrogen sulfide, and nitrogen. Having the K-value of every component in the mixture at three phases (Lw-H-V) equilibrium, the hydrate formation pressure at a given temperature or vice versa. This method is up to the hydrate formation pressure up to 4000 psia for methane, ethane and propane; up to 2000 psia for isobutene and hydrogen sulfide; up to 1000 psia for carbon dioxide. Sloan (1997), mentioned that the accuracy of the K-value method is impressive, considering the fact that the method preceded the knowledge of the crystal structure. Versions of methane, ethane, carbon dioxide and hydrogen sulfide charts, parameters and accuracy are included in Appendix A.

2.7.2.1 Calculation Algorithms

K-Charts are usually used in three methods:

a) Flash

The first type of calculation is basically a flash. The objective is to calculate the amount of phases present in an equilibrium mixture and to determine the composition of the coexisting phase. The temperature, pressure and the compositions are the input parameters.

The objective function to be solved in the Rachford-Rice form is:

$$\boxed{f(V)=\Sigma\frac{z_i(1-K_i)}{1+V(K\ -1)}} \tag{2.21}$$

where z_i is the composition of the feed on water-free basis. Iterations are used to solve for the vapor phase fraction, V, such that the functions equals to zero.
The vapor phase composition can then be computed as follows:

$$\boxed{y_i=\frac{z_iK_i}{1+V(K_i-1)}} \tag{2.22}$$

The composition of solid then can be calculated from:

$$\boxed{s_i=\frac{y_i}{K_i}} \tag{2.23}$$

b) Incipient Solid Formation

The other two methods are incipient solid formation points and are basically equivalent to a dew point. This is a standard hydrate calculation. The purpose of this calculation is:

i) To estimate the pressure if temperature and composition is given

ii) To estimate the temperature if pressure and composition is given

$$\boxed{f_1(T) = 1 - \Sigma \frac{y_i}{K_i}} \qquad (2.24)$$

$$\boxed{f_2(P) = 1 - \Sigma \frac{y_i}{K_i}} \qquad (2.25)$$

Equation 2.24 or 2.25 is chosen depending on whether to calculate pressure or temperature. Iterations are performed on the function until it equals to unity.

CHAPTER 3
RESEARCH METHODOLOGY

The project will be divided to 5 phases in order to ensure the smoothness of the project flow. The first phase will be attributed to understanding of hydrates and its formation, followed by familiarization with the iCON simulation software, temperature and pressure simulation with and without the presence of impurities, hydrate equilibrium condition with the presence of hydrogen sulfide, H_2S and ethane, C_2H_6, and lastly the analysis of data.

3.1 Studies on Hydrates

In order to simulate the formation temperature and pressure of gas hydrates, the properties of hydrate has first to be identified. The properties, conditions for formation, prevention method, calculation method and problems in industry will be covered in this phase.

3.2 Familiarization of iCONS software

ICONS software is Petronas Steady State Simulator which is jointly developed by Petronas Research and Virtual Materials Group. PetronasSim version 2.55.2 that will be used in this work is capable of predicting hydrate formation pressure/temperature gas compositions and water/gas ratio. Hydrate simulation is built based on K-factor method and Advanced-Peng Robinson equation of state. K-factor which originated from Carson and coworkers (1942) is defined as the distribution of component between hydrate and the gas which is available in literature for each of the components commonly encountered in natural gas. In iCONS, Advanced-Peng Robinson is chosen as the property package for the calculation of hydrate formation pressure and temperature due to its stability with all the fluid properties in natural gas.

3.3 Temperature and Pressure Simulation

The temperature and composition of gas and water will be made manipulative variable and pressure will be made the dependent variable. The system will be simulated using water/gas ratio of 5.75 which is the minimum water/gas ratio for Hydrate Structure I when all cages are filled with gas molecules.

3.4 Hydrate equilibrium Condition

The hydrate equilibrium for methane, CH_4 and carbon dioxide, CO_2 will first be studied. Then, hydrogen sulfide, H_2S and ethane, C_2H_6 will be introduced and the effects will be studied.

3.5 Analysis of data

Results of the simulation will be presented and discussed n detail as below in Chapter 4:

i) Effect of temperature on pressure formation of CH_4, CO_2 and H_2S mixture hydrate.

ii) Effect of H_2S content on pressure formation of CH_4 and CO_2 equilibrium hydrate

iii) Effect of temperature on pressure formation of CH_4, CO_2, C_2H_6 and H_2S mixture hydrate.

iv) Effect of H_2S and C_2H_6 content on pressure formation of CH_4 and CO_2 equilibrium hydrate

v) Effect of water gas ratio in feed on pressure formation of CH_4, CO_2, C_2H_6 and H_2S hydrate

vi) Effect of temperature on hydrate phase equilibrium composition of CH_4, CO_2, C_2H_6 and H_2S mixture hydrate

vii) Comparison between iCON and K-Chart Method

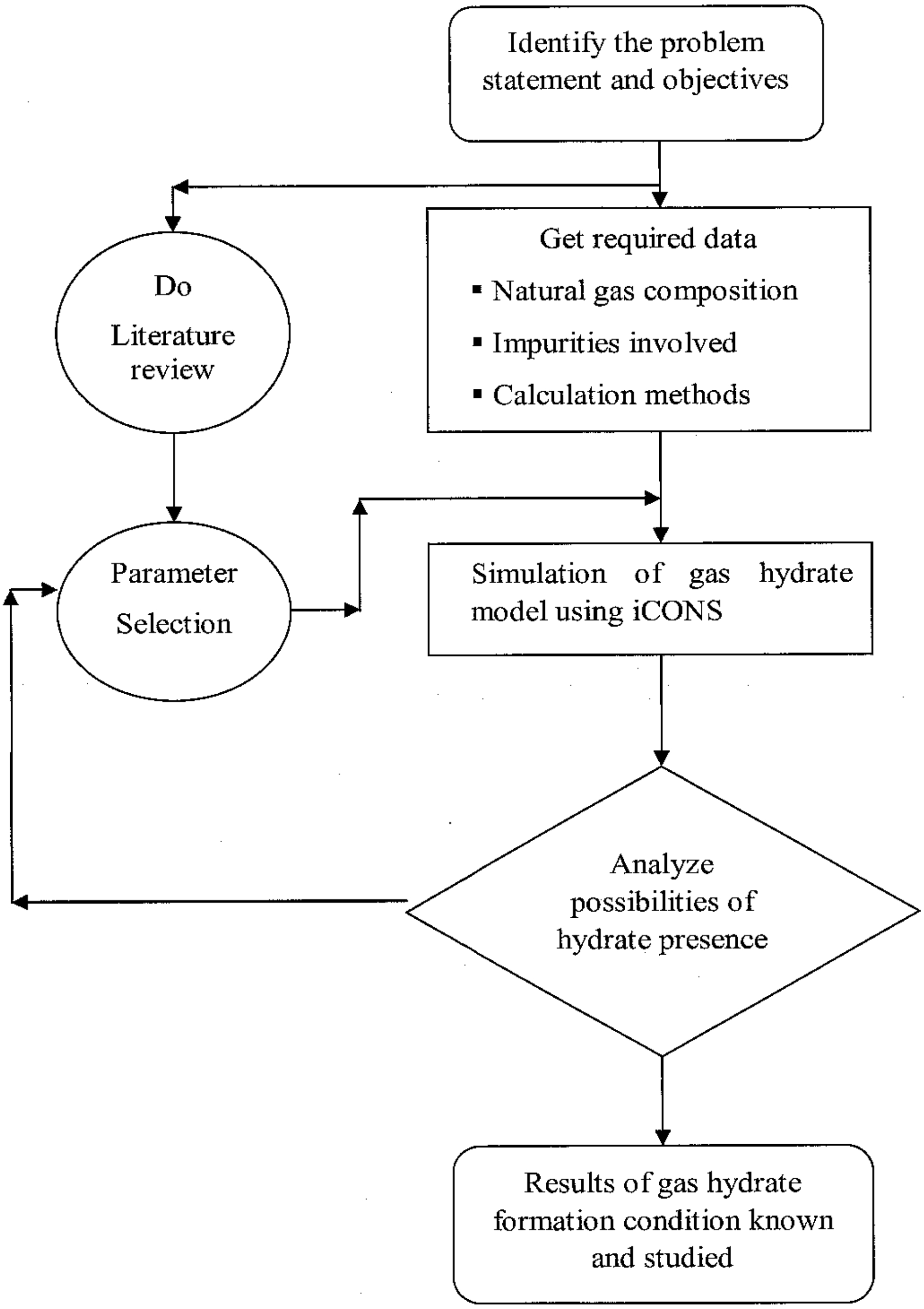

Figure 6 Methodology of the research project

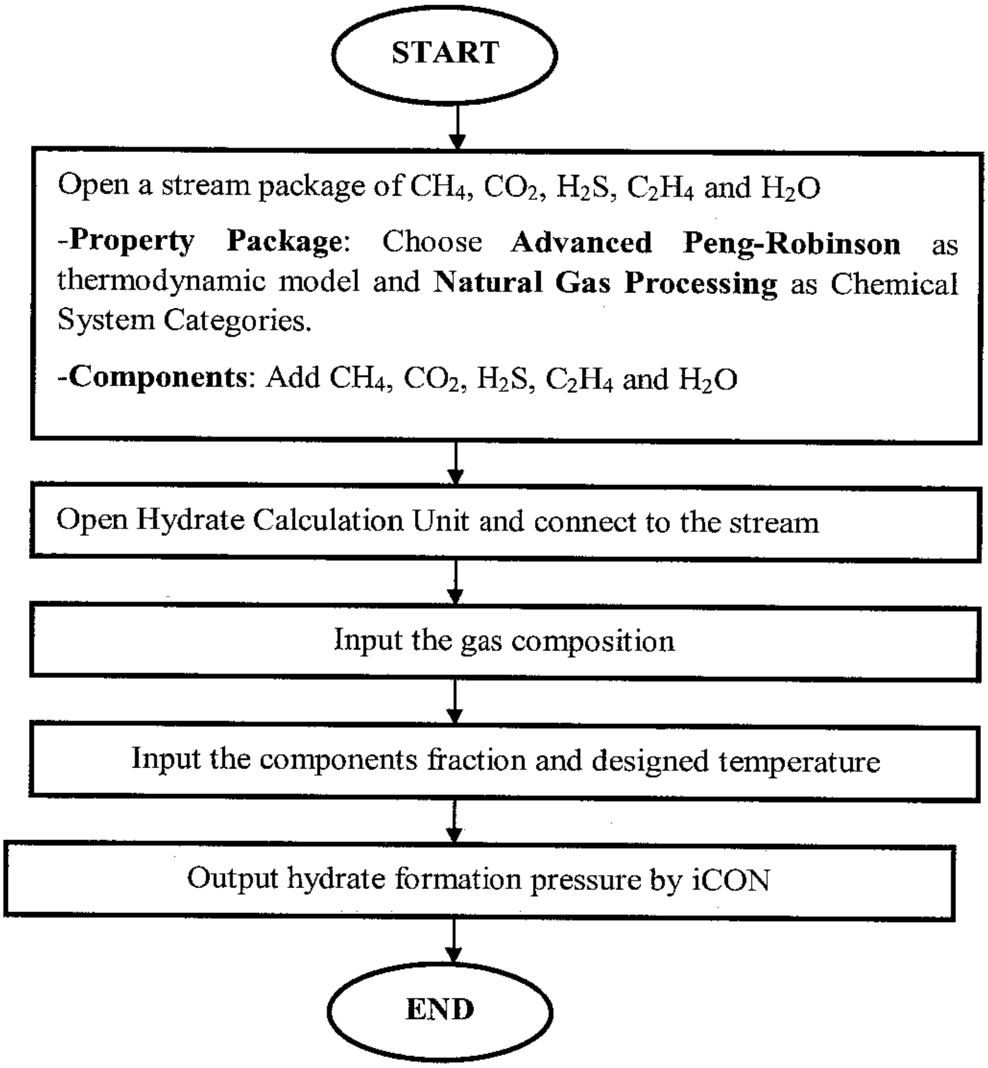

START

Open a stream package of CH_4, CO_2, H_2S, C_2H_4 and H_2O

-**Property Package**: Choose **Advanced Peng-Robinson** as thermodynamic model and **Natural Gas Processing** as Chemical System Categories.

-**Components**: Add CH_4, CO_2, H_2S, C_2H_4 and H_2O

Open Hydrate Calculation Unit and connect to the stream

Input the gas composition

Input the components fraction and designed temperature

Output hydrate formation pressure by iCON

END

Figure 7 Simulation steps in iCON to obtain formation pressure

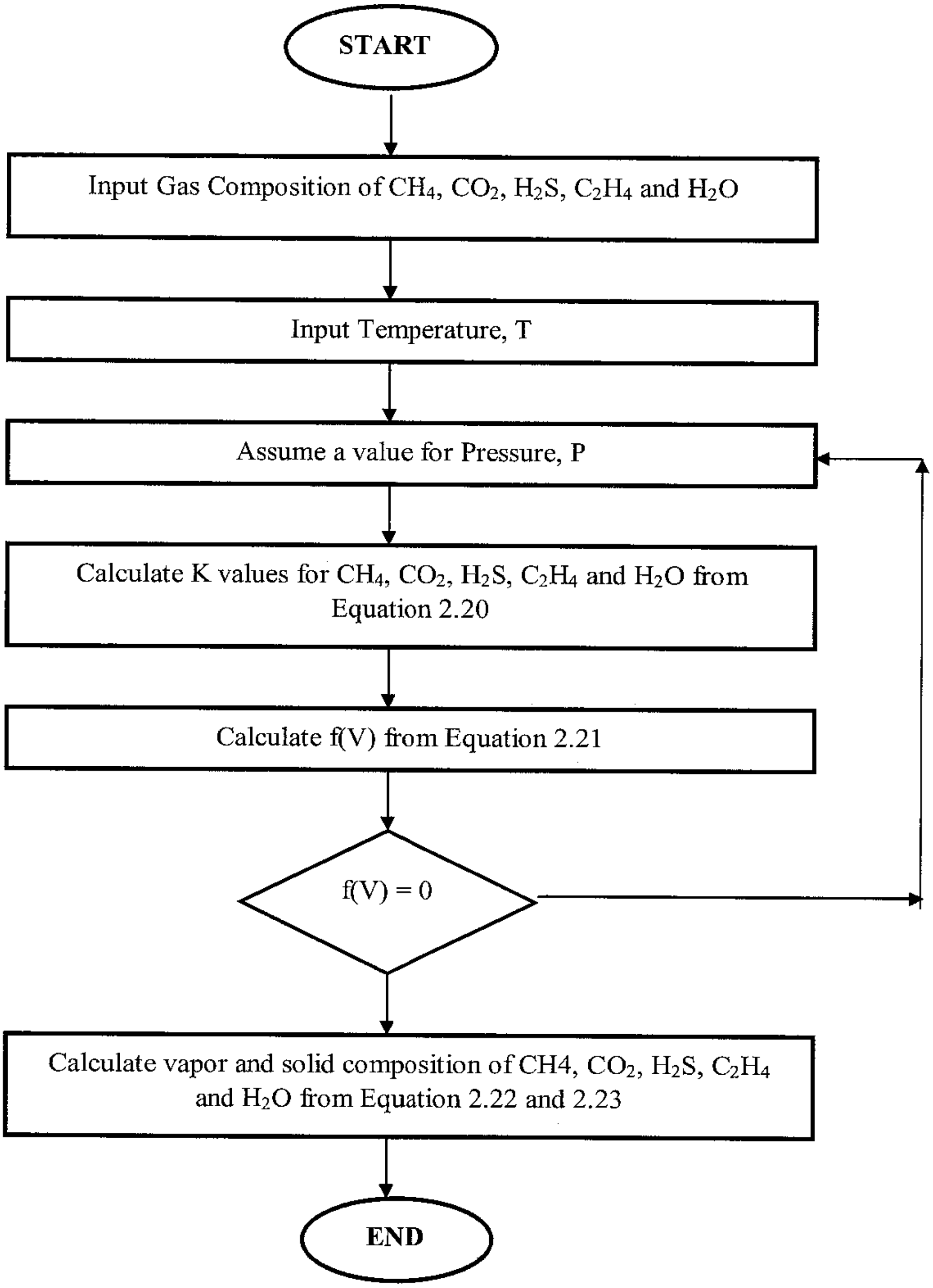

Figure 8 K-Chart method using Excel to obtain hydrate equilibrium composition

CHAPTER 4

RESULT AND DISCUSSION

This section presents the data obtained form the simulation using Petronas iCONs and K-Chart Method which comprises of studies on:

i) Effect of H_2S content on CH_4 hydrates formation.

ii) Effect of C_2H_6 content on CH_4 hydrates formation.

iii) Effect of C_2H_6 and H_2S on CH_4 hydrates formation.

iv) Effect of water gas ratio in feed on formation of CH_4, CO_2, C_2H_6 and H_2S mixture hydrate.

v) Effect of temperature on hydrate phase equilibrium composition of CH_4, CO_2, C_2H_6 and H_2S mixture hydrate

vi) Comparison between iCON and K-Chart Method

4.1 Effect of impurities H_2S, C_2H_6 and combination of H_2S, C_2H_6 on CH_4 hydrate formation

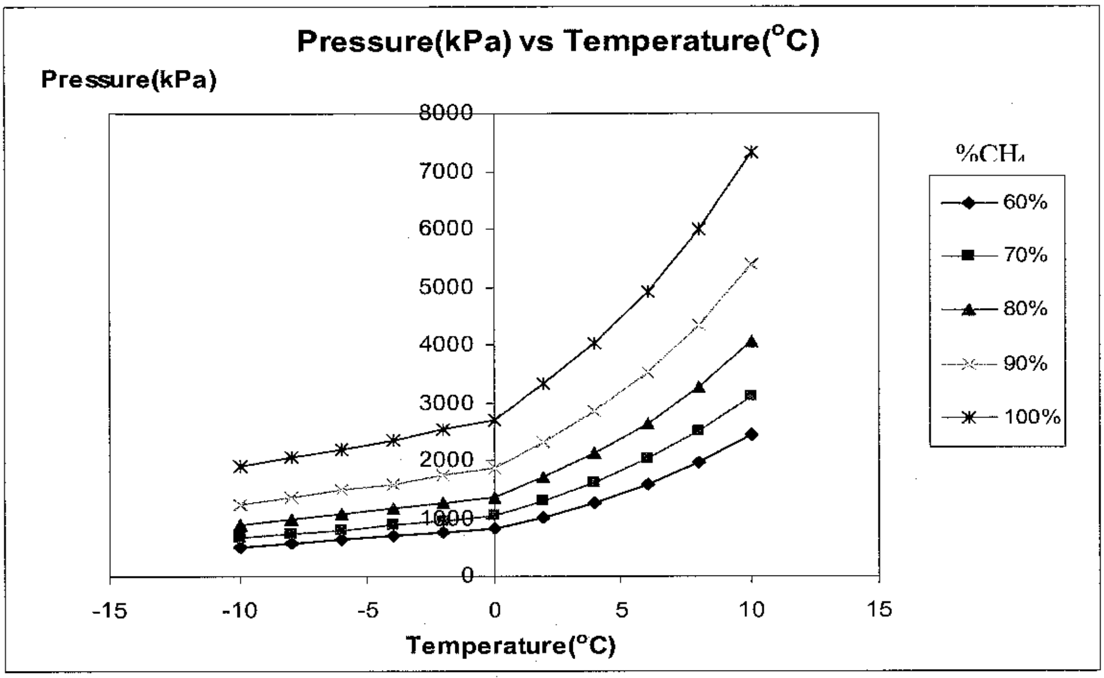

Figure 9 Pressure formation versus temperature for CH_4, CO_2, H_2S (WGR 5.75). (iCON simulation)

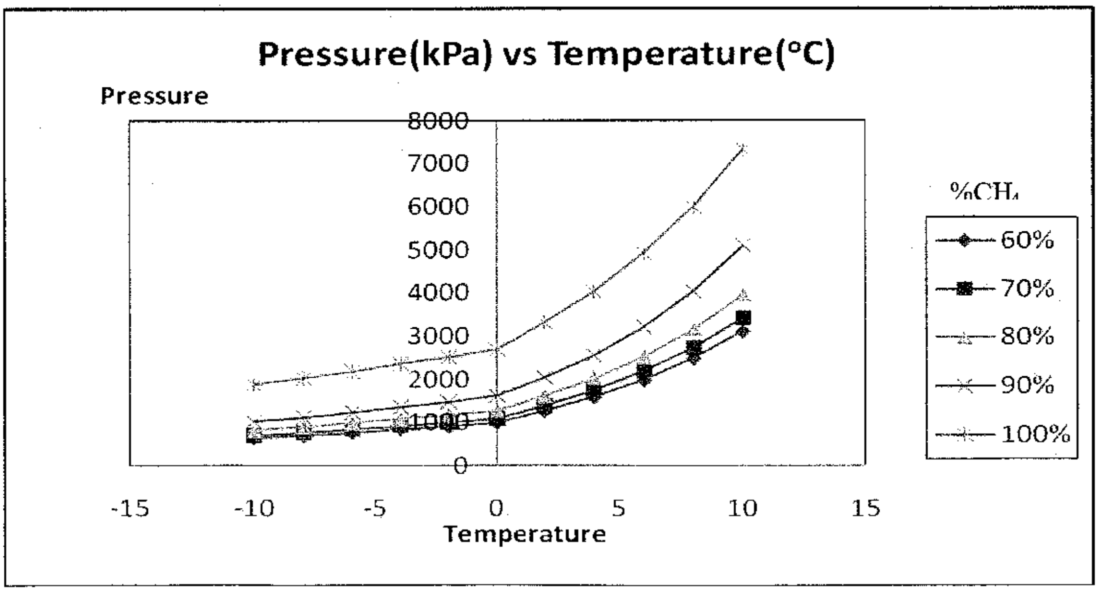

Figure 10 Pressure formation versus temperature for CH_4, CO_2, C_2H_6 (WGR 5.75). (iCON simulation)

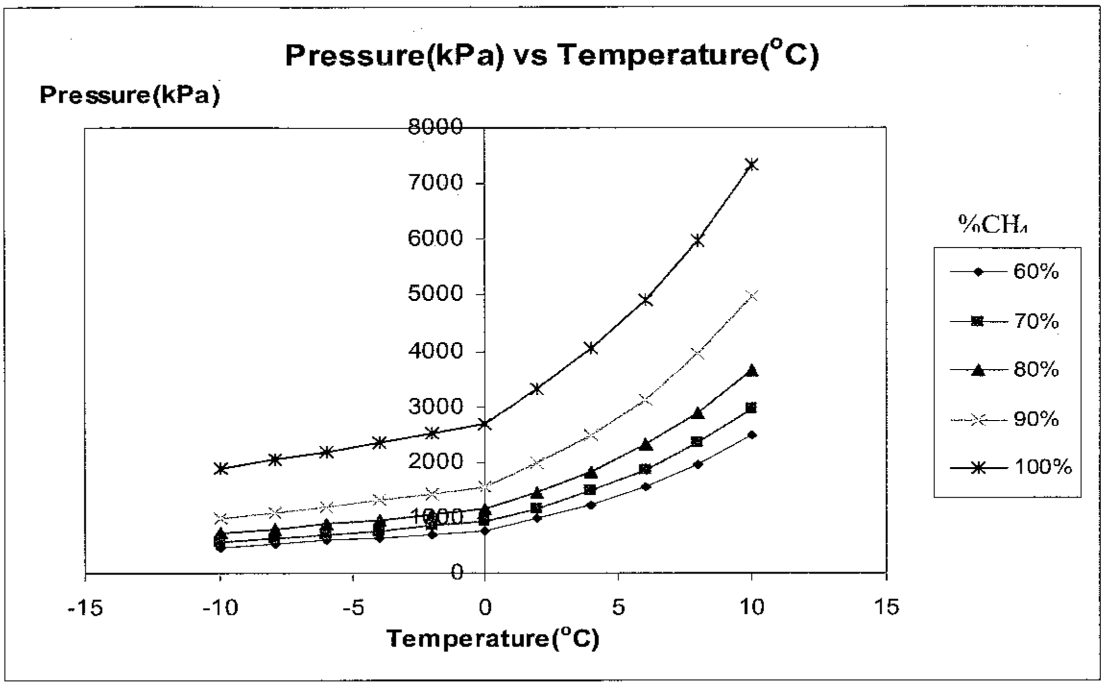

Figure 11 Pressure formation versus temperature for CH_4, CO_2, H_2S, C_2H_6 (WGR 5.75). (iCON simulation)

Figure 9, Figure 10 and Figure 11 shows the plot formation pressure of CH_4 hydrate with impurities, H_2S and C_2H_6 respectively and combination of both at various CH_4 compositions ranging from 60% to 100%. These pressures are obtained from iCON simulation by varying the temperature from -10°C to 10°C. This range of temperature is based on upstream facilities in Saderi platform where studies found that the minimum temperature of seabed is -15°C.

From the positive slope of these three figures, it can be deduced that higher temperature requires higher formation pressure. Below 0°C, the increase in formation pressure is smaller compared to temperature greater than 0°C. The difference can be explained by the change in phase equilibrium. As the temperature increases from negative to positive, the phase changes from I-V-H (Ice-Vapor-Hydrate) to L_w-V-H (Liquid water-Vapor-Hydrate).

Based on the figures, the change of phase equilibrium occurred at 0°C. This finding can be supported by Figure 4, Makagon (1997) where the turning points (quadruple point) for pure CH_4, H_2S, C_2H_6 and CO_2 for P-T Hydrate formation are at 0°C. Thus, this can prove that change of phase at 0°C also applies to mixtures.

The presence of C_2H_6 and H_2S lowers the formation pressure of CH_4 and CO_2 hydrate. In terms of molecular structure level, the reason presence of ethane, C_2H_6 and hydrogen sulfide, H_2S lowers the formation pressure required for hydrate formation at a given temperature is because of structural change. According to Sloan (1997), a big structure of molecules lowers the equilibrium pressure and it is vital for stability. Furthermore, according to GPSA (1998), the presence of $CO_2$and H_2S shifts the equilibrium lines to the right. This results in a decrease in hydrate pressure for a given temperature.

4.2 Effect of Water Gas Ratio (WGR) on pressure formation of CH_4 hydrate with the presence of impurities

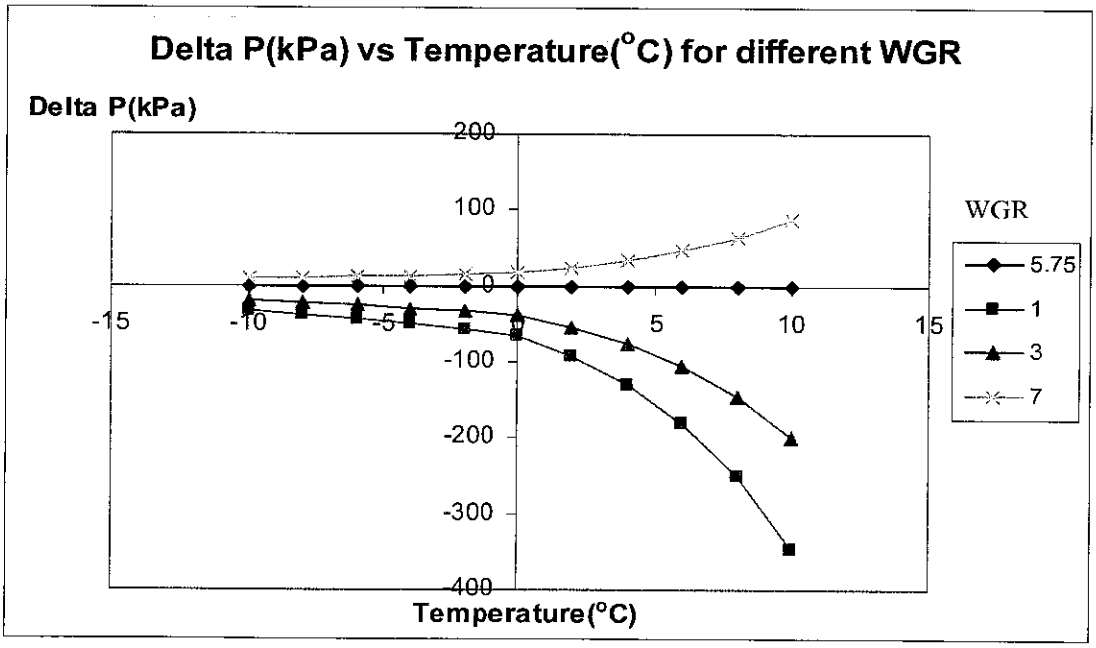

Figure 12 Delta P formation at different WGR to temperature for 80% CH_4, 13.3% CO_2 and 6.7% H_2S (basis WGR=5.75)

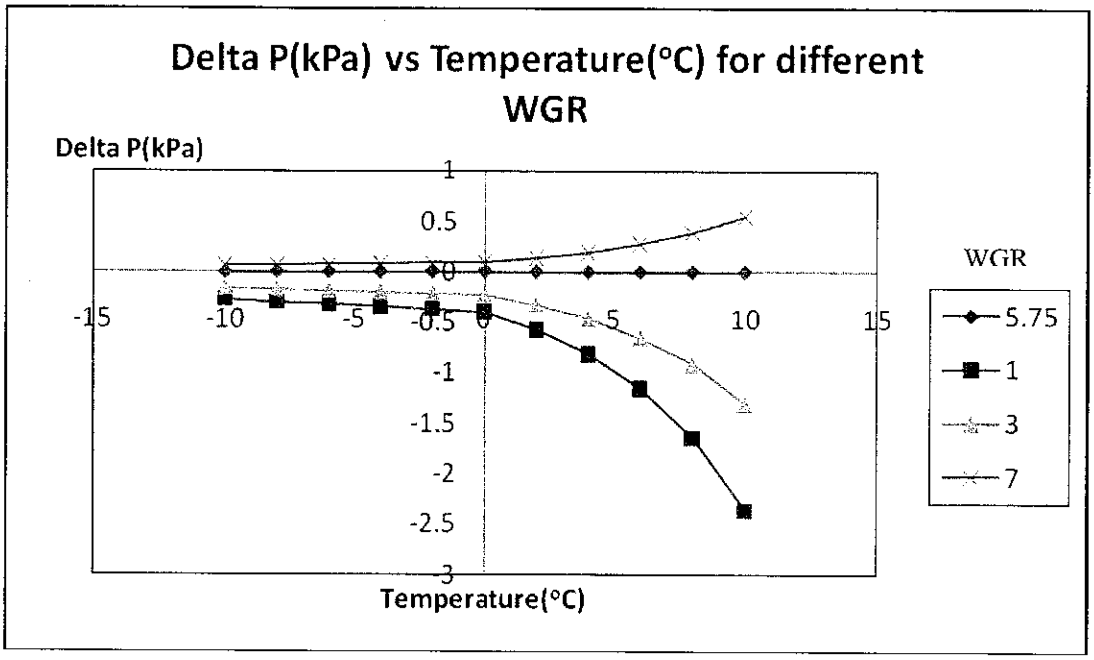

Figure 13 Delta P formation at different WGR to temperature for 80% CH_4, 16% CO_2 and 4% C_2H_6. (basis WGR=5.75)

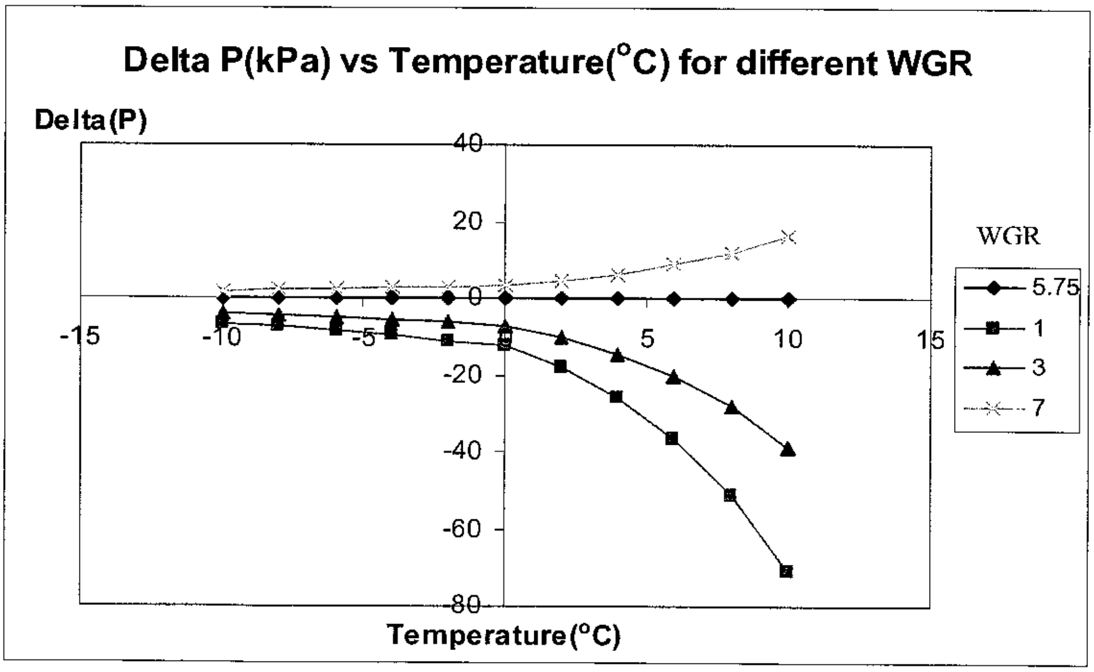

Figure 14 Delta P formation at different WGR to temperature for 80% CH_4, 3.64% CO_2, 14.55% C_2H_6 and 1.82% H_2S. (basis WGR=5.75)

Figure 12, Figure 13 and 14 shows the delta P of h CH_4 hydrate with impurities, H_2S and C_2H_6 respectively and combination of both at various water to gas ratio ranging from 1, 3, 5.75 and 7. According to McCain (2003), the carbon dioxide composition in natural gas is higher than that of hydrogen sulfide, thus a ratio of 2:1 of CO_2 to H_2S is taken. The formation pressure at water to gas ratio of 5.75 is taken as reference pressure because 5.75 is the minimum water to gas ratio that represents the full occupancy of 12-hedral cages of Structure I hydrate. From these figures, it can be seen that delta P of water to gas ratio of 7 is positive whereas the water to gas ratio of 1 and 3 is negative. This concludes that higher water to gas ratio signifies higher formation pressure to form hydrate. According to McCain (1990), the water gas ratio will affect the configuration of hydrate and also determines whether the gas hydrate will form at the condition.

4.3 Effect of Pressure on Hydrate Phase Equilibrium Composition of CH_4 hydrate in the presence of impurities

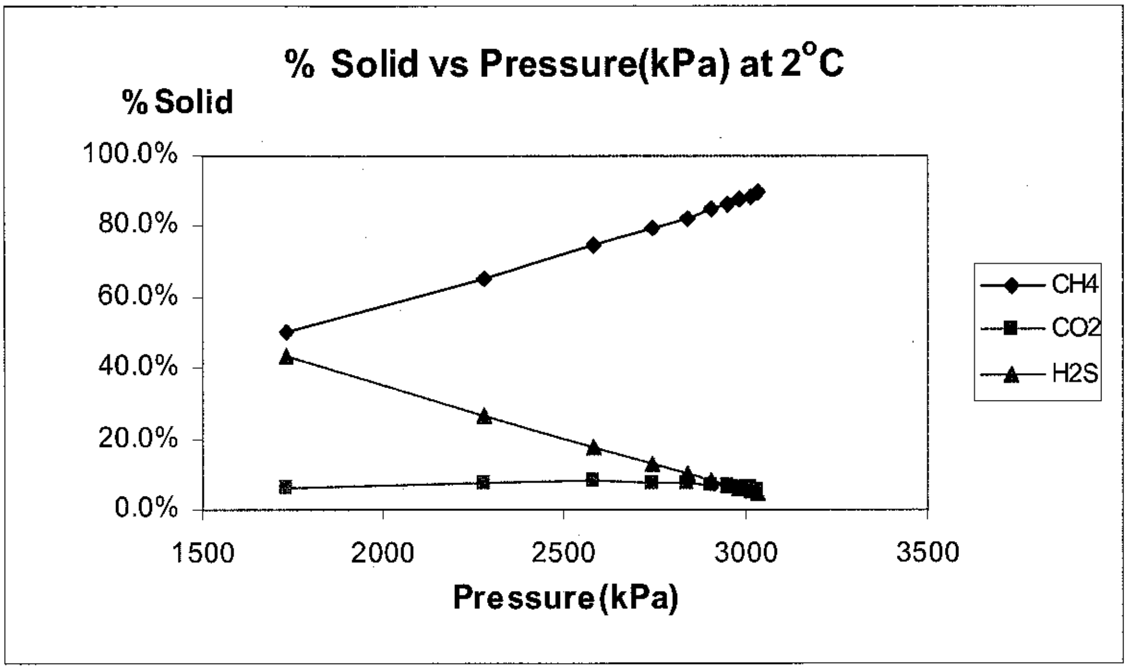

Figure 15 Solid Phase versus Formation Pressure for CH_4, CO_2, H_2S hydrate at 2°C, 80 mol% CH_4. (K-Chart Method)

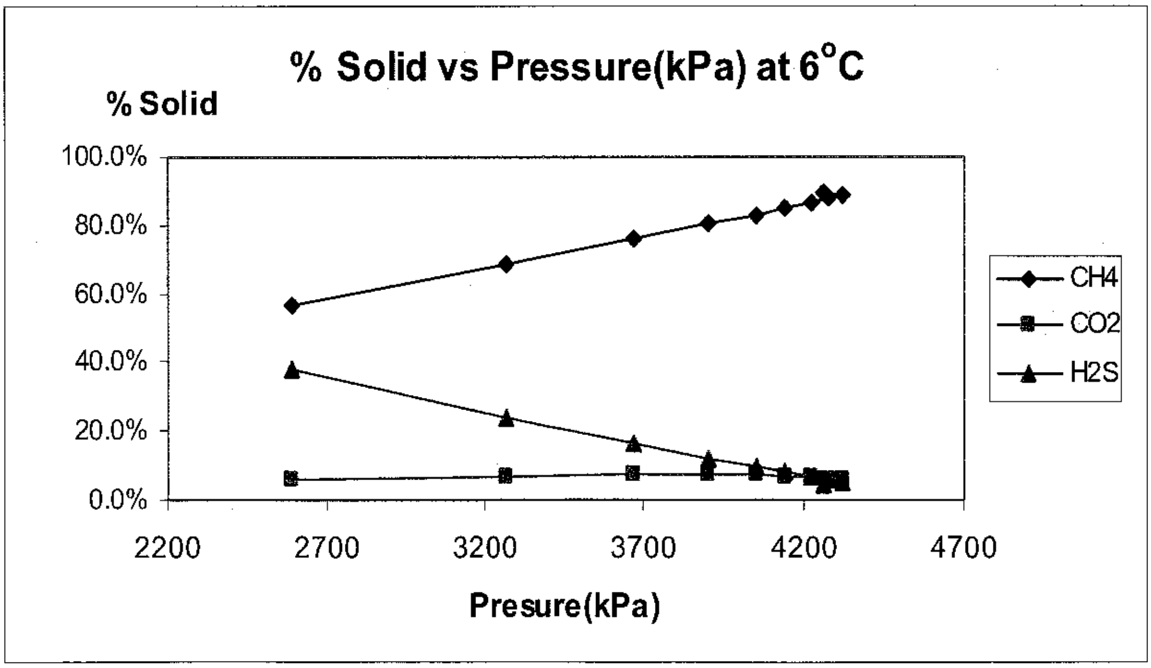

Figure 16 Solid Phase versus Formation Pressure for CH_4, CO_2, H_2S hydrate at 6°C, 80 mol% CH_4. (K-Chart Method)

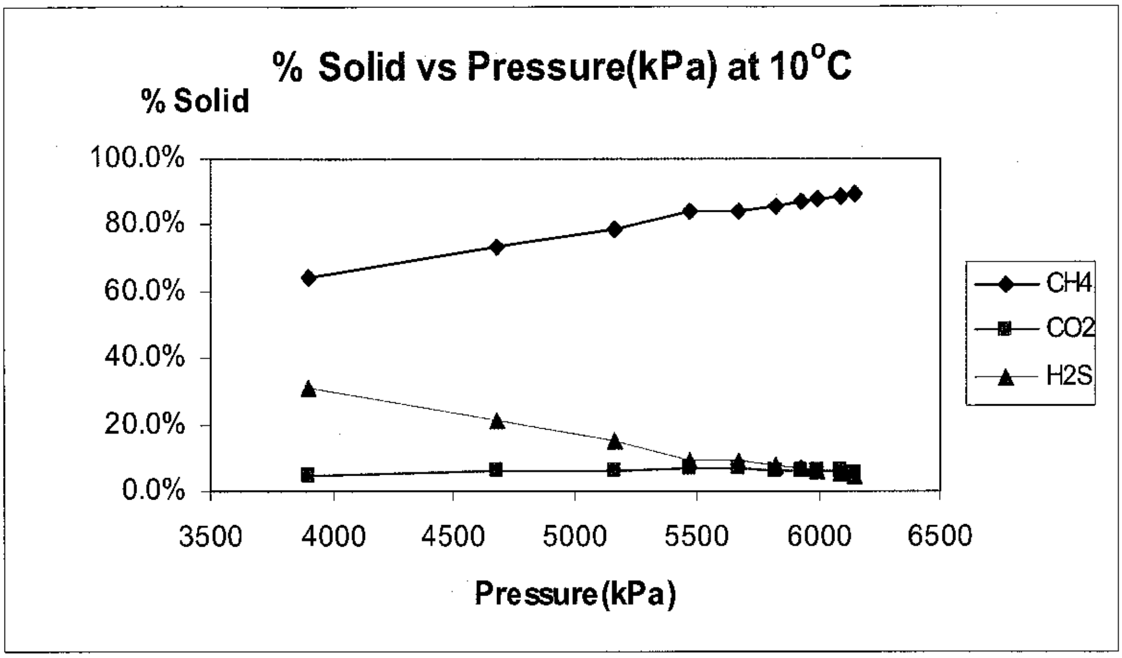

Figure 17 Solid Phase versus Formation Pressure for CH_4, CO_2, H_2S hydrate at 10°C, 80 mol% CH_4. (K-Chart Method)

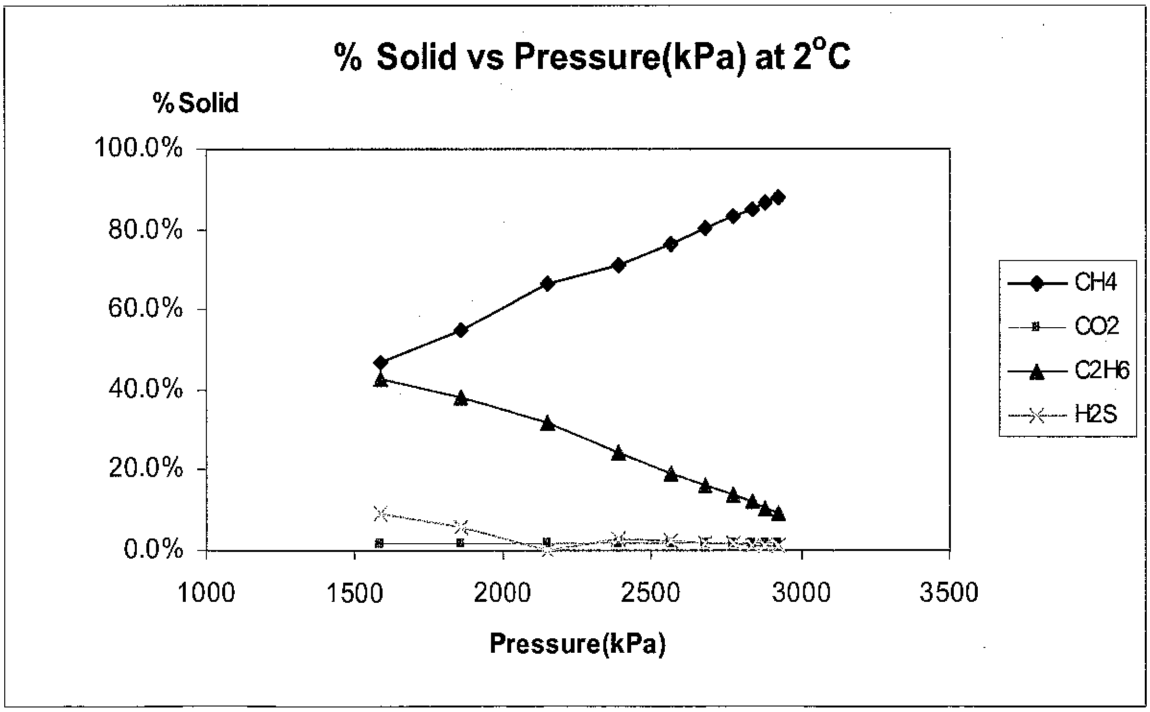

Figure 18 Solid Phase versus Formation Pressure for CH_4, CO_2, H_2S, C_2H_6 hydrate at 2°C, 80 mol% CH_4. (K-Chart Method)

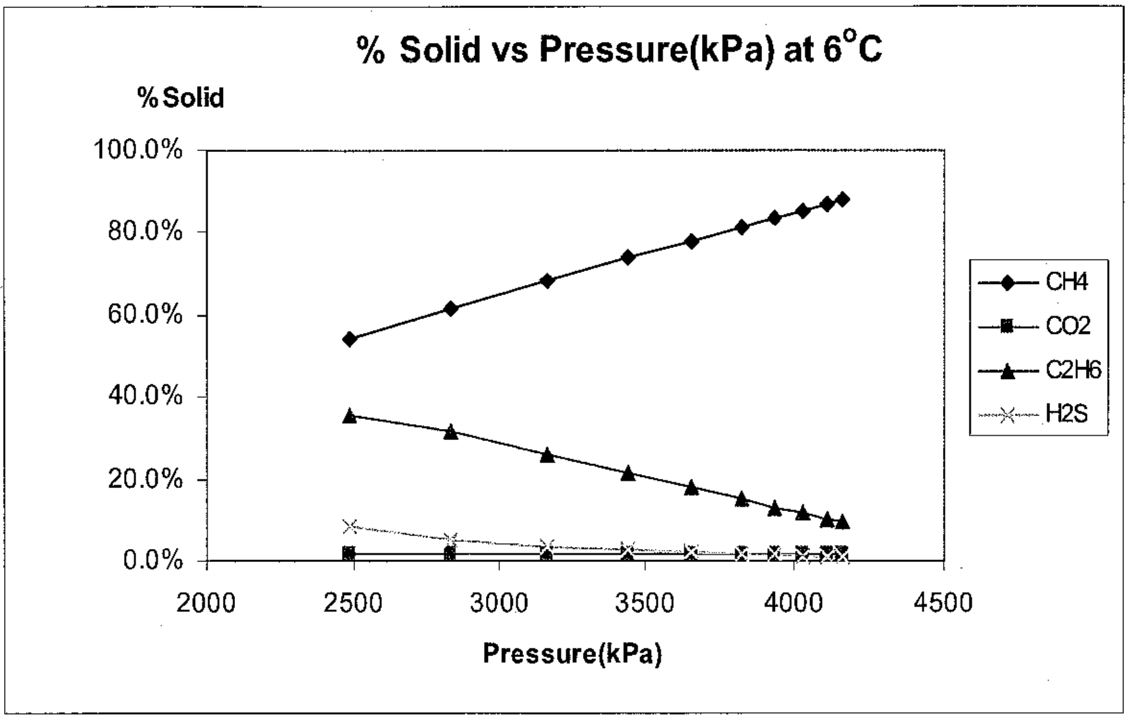

Figure 19 Solid Phase versus Formation Pressure for CH_4, CO_2, H_2S, C_2H_6 hydrate at 6°C, 80 mol% CH_4. (K-Chart Method)

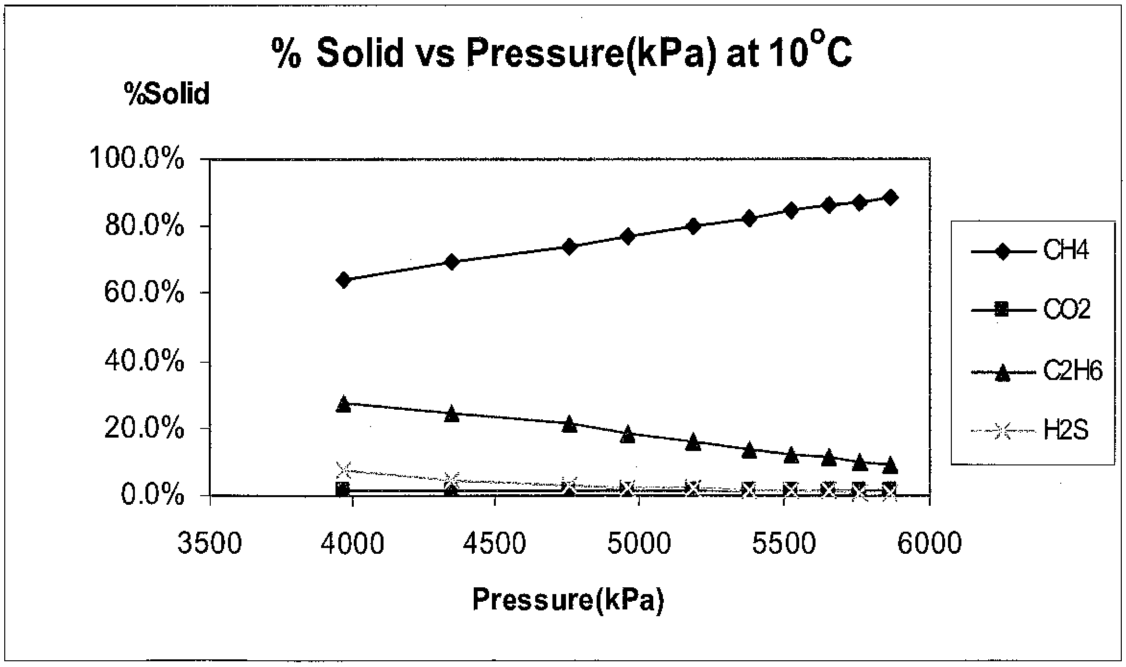

Figure 20 Solid Phase versus Formation Pressure for CH_4, CO_2, H_2S, C_2H_6 hydrate at 10°C, 80 mol% CH_4. (K-Chart Method)

As pressure increases, H_2S and C_2H_6 content in the solid (hydrate) decreases as shown in the graphs (Figure 15 to 20). The decrement corresponds to the increment of CH_4 content in the hydrate. This reduction of impurity phase is because as pressure increases, more CH_4 will be incorporated into hydrate lattice and be distributed into two phases.

4.4 Comparison for iCON and K-Chart Method Calculation at 80 mol% Methane

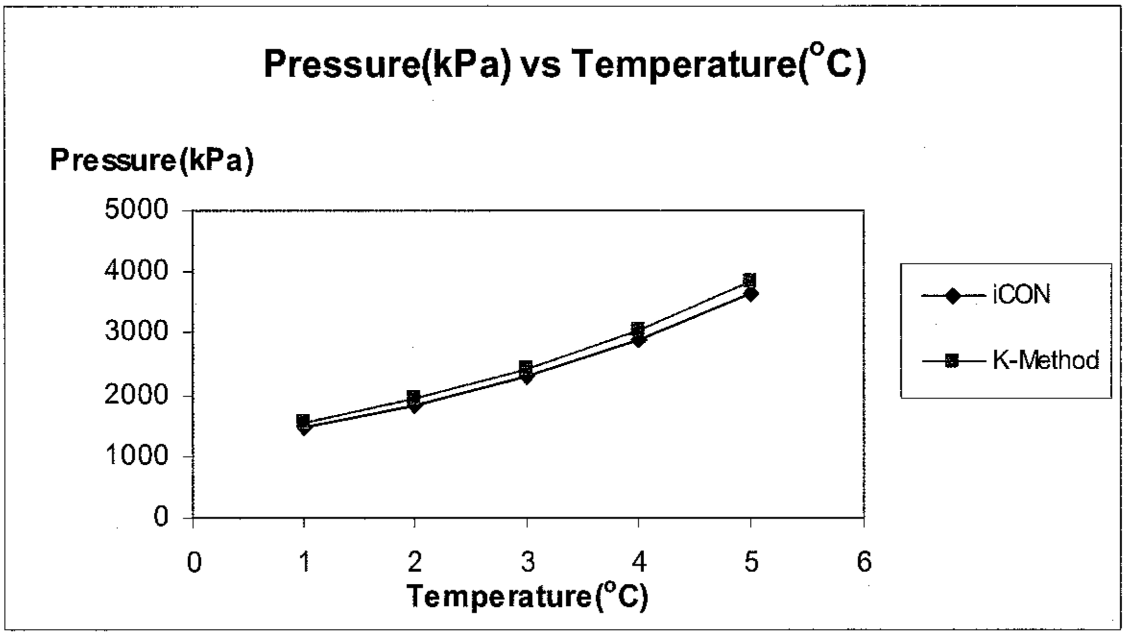

Figure 21 Comparison for iCON and K-Chart Method Calculation for 80 mol% Methane.

Figure 21 shows the comparison for pressure formation obtained from iCON simulation and iterations by K-Chart Method. There is not much deviation between these two methods proves the reliability of the simulation results as Sloan (1997) mentioned that the accuracy of K-Chart method is impressive, considering the fact that the method preceded the knowledge of the crystal structure and thus the K-Chart Method can be used as a reference.

CHAPTER 5

CONCLUSION AND RECOMMENDATION

In conclusion, the objectives of this research have been achieved as the author has managed to explore the effect of hydrogen sulfide and ethane in the equilibrium conditions of hydrate formation, effect of temperature and pressure governing the formation of the hydrate in the presence of the targeted impurities, effect of water gas ratio in feed on pressure formation of CH_4, CO_2, C_2H_6 and H_2S hydrate, effect of water gas ratio in feed on pressure formation of CH_4, CO_2, C_2H_6 and H_2S hydrate and the effect of temperature on hydrate phase equilibrium composition of CH_4, CO_2, C_2H_6 and H_2S mixture hydrate.

For gas hydrate formation at higher temperature requires higher pressure. Hydrate occurred during many working conditions for example while drilling and producing the natural gas form the well or while processing and transporting in the pipeline. Therefore, it is recommended that the upstream facilities be operated at optimum temperature and pressure.

The presence of CO_2, C_2H_6 and H_2S lowers the hydrate formation pressure. In terms of molecular structure level, the reason presence of ethane, C_2H_6 and hydrogen sulfide, H_2S lowers the formation pressure required for hydrate formation at a given temperature is because of structural change. This is because a big structure of molecules lowers the equilibrium pressure and it is vital for stability. Higher water to gas ratio signifies higher formation pressure to form hydrate. As pressure increases, H_2S and C_2H_6 content in the solid (hydrate) decreases. ICON simulation and K-Chart Method shows good compromise as the difference between these two methods are small.

The compositions and natural gas, specifically in this case, CO_2, C_2H_6 and H_2S should be taken into high consideration as according to Sloan (1997), hydrate prevention is necessary in the oil and gas industry as the prevention of hydrate formation requires substantial investment; as much as up to 10 to 15% of the production cost. Removal of continuous hydrate plugs from an onshore well costs up to $1 million, and from an offshore pipeline, $2 to 4 million.

REFERENCES

Yuri F. Makagon 1997, *Hydrates of Hydrocarbon*, Tulsa, Oklahoma, PennWell Publishing.

Sloan E.D.Jr 1997, *Clathrates Hydrates of Natural Gases*, 2nd Ed, New York, Marcel Dekker.

Sloan E.D.Jr 2000, *Hydrates Engineering*, Volume 21, Texas, Society of Petroleum Engineers Inc.

Carroll D.B 2003, *Natural Gas Hydrates: A Guide for Engineers*, Amsterdam, Gulf Professional Publishing.

Michael D.Max et al 2006, *Economic Geology of Natural Gas Hydrate*, Vol 9, Netherlands, Springer.

Gutt C. et al 2000, *The Structure of Deuterated Methane Hydrate*, Journal Chemical Physics, 113, 4713-4122.

Smith, J.M. et al, 2005, *Introduction to Chemical Engineering Thermodynamics*, Mc Graw Hill, Singapore

Danesh, Ali,, 1998, *PVT and Phase Behavior of Petroleum Reservoir Fluids*, Elsevier Science, Netherlands

Elliot, Richard et al, 1999, *Introductory Chemical Engineering Thermodynamics*, Prentice Hall, New York

Vu Thi Huong, 2005, *Removal of Carbon Dioxide from Natural Gas by using Gas Hydrate*, Universiti Teknologi Petronas

Vu Thi Huong, Hilmi Mukthar, Prof. Dr. Thanabalan Murugesan, *Thermodynamic Properties of Methane Hydrate*, Universiti Teknologi Petronas

Gas Tracers, 21 August 2008

<http://www.gaschem.com/gashydrates.html>

Union Gas, 4 September 2008

<http://www.uniongas.com/default.asp>

Gas Hydrate Research

<http://www.pet.hw.ac/uk/research/hydrate>

APPENDICES

APPENDIX A

K-VALUE CHARTS

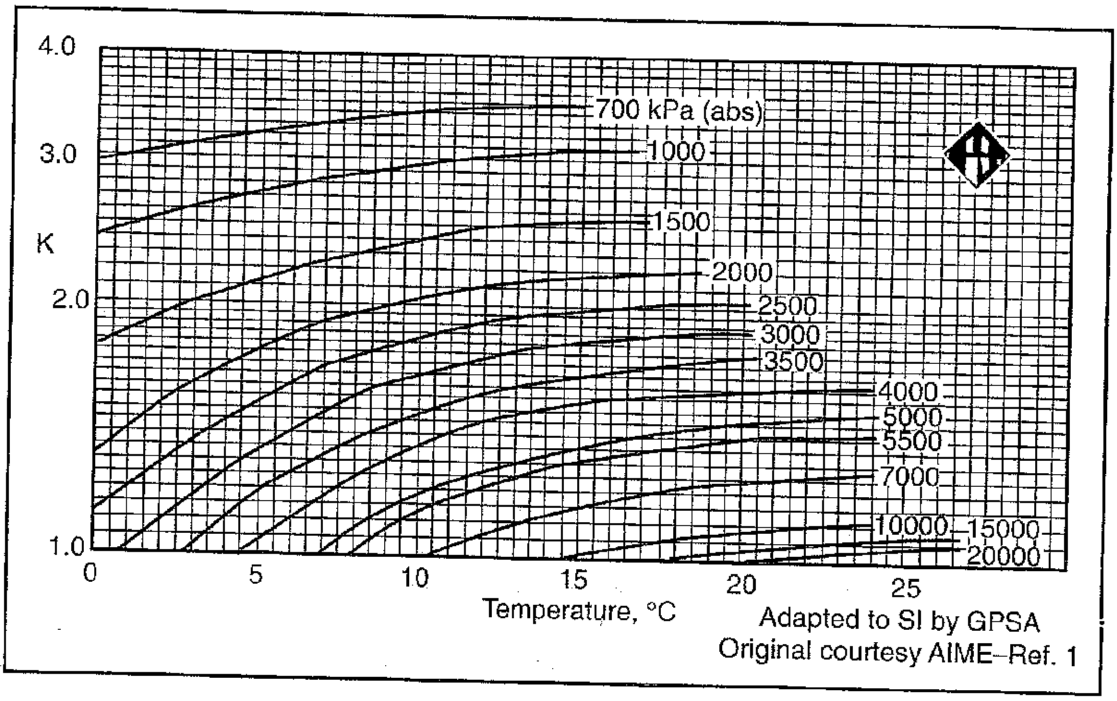

K-Equilibrium constant for Methane (GPSA, 1998)

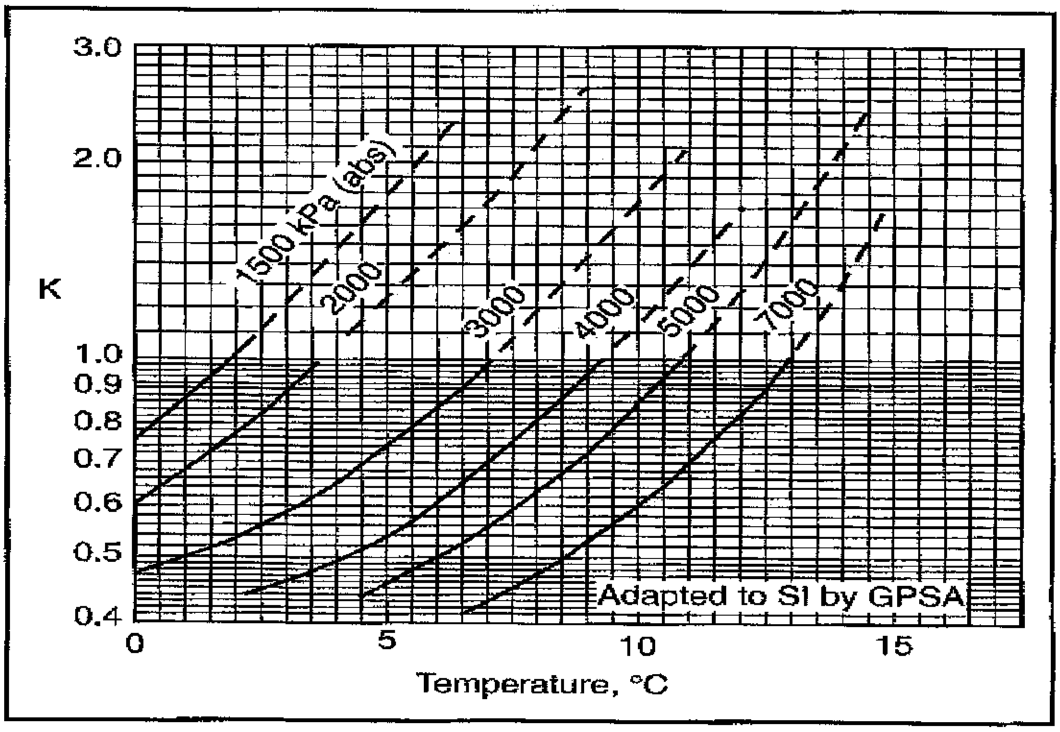

K-Equilibrium constant for Carbon dioxide (GPSA, 1998)

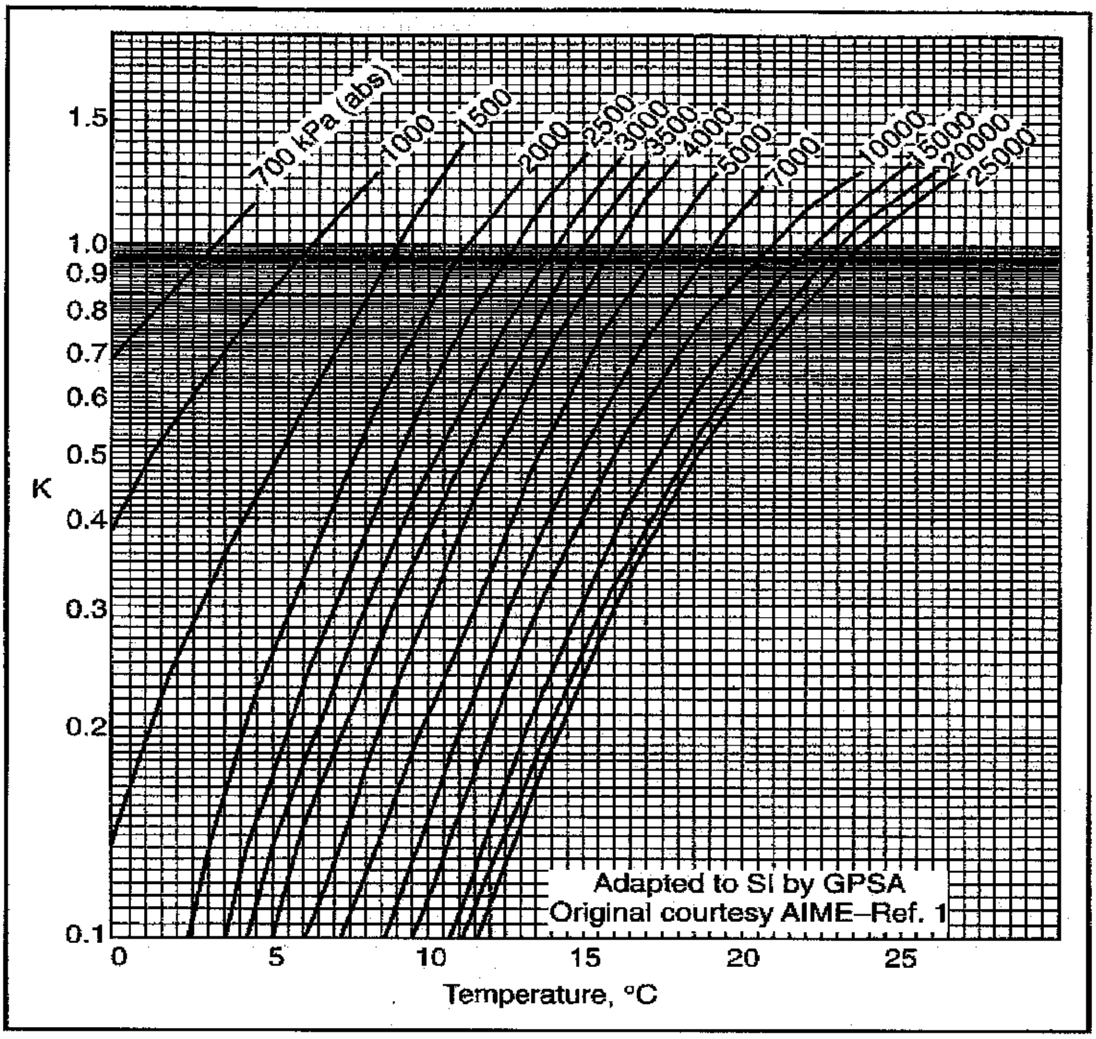

K Equilibrium constant for Ethane (GPSA, 1998)

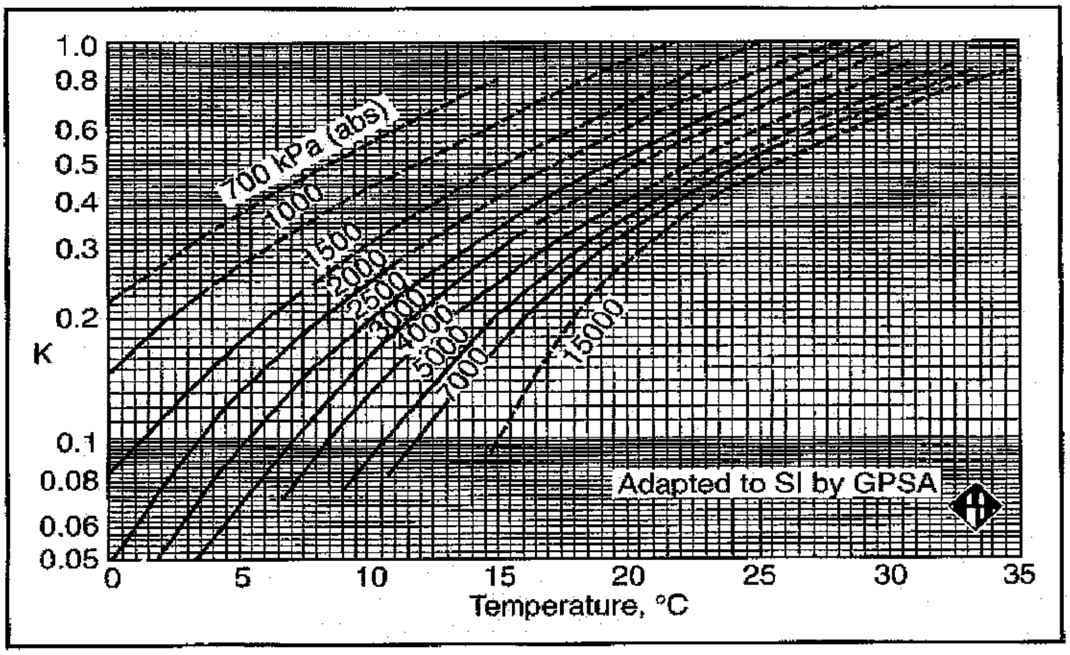

K Equilibrium constant for Hydrogen Sulfide (GPSA, 1998)

K-VALUE CONSTANTS

Component	Methane	Carbon Dioxide	Ethane	Hydrogen Sulfide
A	1.63636	9.0242	6.41934	-4.707100
B	0	0	0	0.061920
C	0	0	0	0
D	31.6621	-207.033	-290.283	82.627000
E	-49.3534	0	2629.10	0
F	-0.00000531	0.0000466	0	-0.000007
G	0	-0.006992	0	0
H	0	-0.00000289	-0.00000009	0
I	0.128525	-0.006223	0.129759	0.240869
J	-0.78338	0	-1.19703	-0.644050
K	0	0	-84600	0
L	0	0	-71.0352	0
M	0	0.27098	0.596404	0
N	-5.3569	0	-4.7437	-12.704000
O	0	0	78200	0
P	-2.3E-07	0.0000882	0	-0.000001
Q	-2E-08	0.00000255	0	0
R	0	0	0	0
Correlation Coefficient	0.999	0.996	0.998	0.999000

K Value constants for Methane, Carbon Dioxide, Ethane and Hydrogen Sulfide (GPSA, 1998)

APPENDIX B

ICON SIMULATION RESULTS

Table B1:Hydrate temperature and pressure formation for CH_4, CO_2, H_2S (WGR 5.75)

Composition	T(°C)	P(kPa)	Composition	T(°C)	P(kPa)	Composition	T(°C)	P(kPa)
	-10	522.03508		-10	670.1463		-10	889.1352
60% CH_4	-8	575.44928	70% CH_4	-8	737.4392	80% CH_4	-8	975.5701
	-6	632.41049		-6	809.0382		-6	1067.169
26.7% CO_2	-4	692.95074	26.7% CO_2	-4	884.9587	13.3% CO_2	-4	1163.901
	-2	757.07958		-2	965.1866		-2	1265.695
13.3% H_2S	0	824.78208	13.3% H_2S	0	1049.674	6.7% H_2S	0	1372.435
	2	1029.4349		2	1310.763		2	1713.056
	4	1277.8847		4	1626.549		4	2121.864
	6	1585.3789		6	2017.947		6	2628.274
	8	1967.5633		8	2505.421		8	3258.94
	10	2445.4849		10	3116.724		10	4050.282

Table B2:Hydrate temperature and pressure formation for CH_4, CO_2, H_2S (WGR 5.75)

Composition	T(°C)	P(kPa)	Composition	T(°C)	P(kPa)
	-10	1244.5981		-10	1901.5141
90% CH_4	-8	1357.9983	100% CH_4	-8	2049.6528
	-6	1477.298		-6	2203.5946
6.7% CO_2	-4	1602.3591	0% CO_2	-4	2363.0599
	-2	1732.9922		-2	2527.7168
3.3% H_2S	0	1868.9637	0% H_2S	0	2697.1892
	2	2325.806		2	3323.646
	4	2865.4882		4	4041.3997
	6	3530.9055		6	4916.7678
	8	4356.1163		8	5991.5142
	10	5387.8474		10	7322.6481

Table B3:Hydrate temperature and pressure formation for CH_4, CO_2, H_2S (WGR 1)

Composition	T(°C)	P(kPa)	Composition	T(°C)	P(kPa)	Composition	T(°C)	P(kPa)
	-10	506.1031		-10	648.55253		-10	856.1262
60% CH_4	-8	556.63192	70% CH_4	-8	712.13333	80% CH_4	-8	937.3389
	-6	610.31829		-6	779.55874		-6	1023.16
26.7% CO_2	-4	667.1671	26.7% CO_2	-4	850.82509	13.3% CO_2	-4	1113.545
	-2	727.16116		-2	925.89266		-2	1208.411
13.3% H_2S	0	790.26474	13.3% H_2S	0	1004.6993	6.7% H_2S	0	1307.643
	2	978.80856		2	1245.338		2	1620.026
	4	1204.8776		4	1533.2855		4	1991.599
	6	1480.5581		6	1885.6357		6	2446.902
	8	1817.566		8	2318.4219		8	3007.63
	10	2231.2813		10	2853.1406		10	3703.433

Table B4:Hydrate temperature and pressure formation for CH_4, CO_2, H_2S (WGR 1)

Composition	T(°C)	P(kPa)	Composition	T(°C)	P(kPa)
	-10	1204.6087		-10	1901.5141
90% CH_4	-8	1312.6455	100% CH_4	-8	2049.6528
	-6	1426.1641		-6	2203.5946
6.7% CO_2	-4	1545.0433	0% CO_2	-4	2363.0599
	-2	1669.1099		-2	2527.7168
3.3% H_2S	0	1798.1476	0% H_2S	0	2697.1892
	2	2226.6384		2	3323.646
	4	2731.0783		4	4041.3997
	6	3350.0683		6	4916.7678
	8	4114.4964		8	5991.5142
	10	5067.1599		10	7322.6481

Table B5:Hydrate temperature and pressure formation for CH_4, CO_2, H_2S (WGR 3)

Composition	T(°C)	P(kPa)	Composition	T(°C)	P(kPa)	Composition	T(°C)	P(kPa
	-10	512.22073		-10	656.21538		-10	869.876
60% CH_4	-8	563.84939	70% CH_4	-8	721.11095	80% CH_4	-8	953.283
	-6	618.78308		-6	790.01685		-6	1041.53
26.7% CO_2	-4	677.03723	26.7% CO_2	-4	862.93242	13.3% CO_2	-4	1134.
	-2	738.60495		-2	939.83094		-2	1232.39
13.3% H_2S	0	803.4562	13.3% H_2S	0	1020.6545	6.7% H_2S	0	1334.80
	2	998.10698		2	1268.5344		2	1659.14
	4	1232.6452		4	1566.3535		4	2046.56
	6	1520.3413		6	1932.5768		6	2523.77
	8	1874.3934		8	2384.8485		8	3114.7
	10	2312.3199		10	2946.9653		10	3852.18

Table B6:Hydrate temperature and pressure formation for CH_4, CO_2, H_2S (WGR 3)

Composition	T(°C)	P(kPa)	Composition	T(°C)	P(kPa)
	-10	1221.9362		-10	1901.5141
90% CH_4	-8	1332.3237	100% CH_4	-8	2049.6528
	-6	1448.3864		-6	2203.5946
6.7% CO_2	-4	1569.9942	0% CO_2	-4	2363.0599
	-2	1696.9694		-2	2527.7168
3.3% H_2S	0	1829.0931	0% H_2S	0	2697.1892
	2	2270.1844		2	3323.646
	4	2790.4617		4	4041.3997
	6	3430.5309		6	4916.7678
	8	4222.8903		8	5991.5142
	10	5212.3286		10	7322.6481

Table B7:Hydrate temperature and pressure formation for CH_4, CO_2, H_2S (WGR 7)

Composition	T(°C)	P(kPa)	Composition	T(°C)	P(kPa)	Composition	T(°C)	P(kPa)
	-10	526.53525		-10	676.57535		-10	898.0478
60% CH_4	-8	580.77773	70% CH_4	-8	744.97583	80% CH_4	-8	985.8613
	-6	638.68031		-6	817.81822		-6	1078.979
26.7% CO_2	-4	700.28315	26.7% CO_2	-4	895.12472	13.3% CO_2	-4	1177.372
	-2	765.60446		-2	976.88635		-2	1280.967
13.3% H_2S	0	834.6338	13.3% H_2S	0	1063.06	6.7% H_2S	0	1389.649
	2	1043.9613		2	1330.2414		2	1737.597
	4	1298.9261		4	1654.2913		4	2155.913
	6	1615.6991		6	2057.2193		6	2675.162
	8	2011.0702		8	2560.7128		8	3323.057
	10	2507.7053		10	3194.2034		10	4137.389

Table B8:Hydrate temperature and pressure formation for CH_4, CO_2, H_2S (WGR 7)

Composition	T(°C)	P(kPa)	Composition	T(°C)	P(kPa)
	-10	1254.3867		-10	1901.5141
90% CH_4	-8	1369.0687	100% CH_4	-8	2049.6528
	-6	1489.7383		-6	2203.5946
6.7% CO_2	-4	1616.2528	0% CO_2	-4	2363.0599
	-2	1748.4165		-2	2527.7168
3.3% H_2S	0	1885.9883	0% H_2S	0	2697.1892
	2	2349.3889		2	3323.646
	4	2897.0161		4	4041.3997
	6	3572.6432		6	4916.7678
	8	4410.8661		8	5991.5142
	10	5459.0423		10	7322.6481

Table B9:Hydrate temperature and pressure formation for CH_4, CO_2, C_2H_6, H_2S (WGR 5.75)

Composition	T(°C)	P(kPa)	Composition	T(°C)	P(kPa)	Composition	T(°C)	P(kPa)
	-10	474.12615		-10	574.80481		-10	723.2558
60% CH_4	-8	526.45577	70% CH_4	-8	636.87484	80% CH_4	-8	799.5295
	-6	582.49808		-6	703.22724		-6	880.9393
7.3% CO_2	-4	642.27348	5.5% CO_2	-4	773.88159	3.6% CO_2	-4	967.5103
	-2	705.77148		-2	848.82369		-2	1059.231
29.1% C_2H_6	0	772.94708	21.8% C_2H_6	0	928.00279	14.6% C_2H_6	0	1156.048
	2	983.66521		2	1178.1196		2	1464.693
3.6% H_2S	4	1242.225	2.7% H_2S	4	1483.6188	1.8% H_2S	4	1839.968
	6	1565.0548		6	1864.7987		6	2308.884
	8	1969.6714		8	2342.7053		8	2898.694
	10	2480.0803		10	2946.6064		10	3648.28

Table B10:Hydrate temperature and pressure formation for CH_4, CO_2, H_2S (WGR 5.75)

Composition	T(°C)	P(kPa)	Composition	T(°C)	P(kPa)
	-10	992.25285		-10	1901.5141
90% CH_4	-8	1094.1069	100% CH_4	-8	2049.6528
	-6	1202.6762		-6	2203.5946
1.8% CO_2	-4	1318.0058	0% CO_2	-4	2363.0599
	-2	1440.0951		-2	2527.7168
7.3% C_2H_6	0	1568.8935	0% C_2H_6	0	2697.1892
	2	1986.4662		2	3323.646
0.9% H_2S	4	2491.787	0% H_2S	4	4041.3997
	6	3127.0672		6	4916.7678
	8	3933.912		8	5991.5142
	10	4974.3377		10	7322.6481

Table B11:Hydrate temperature and pressure formation for CH_4, CO_2, C_2H_6, H_2S (WGR 1)

Composition	T(°C)	P(kPa)	Composition	T(°C)	P(kPa)	Composition	T(°C)	P(kPa)
	-10	468.59693		-10	568.58552		-10	716.7474
60% CH_4	-8	519.95821	70% CH_4	-8	629.63482	80% CH_4	-8	792.0222
	-6	574.91913		-6	694.85779		-6	872.3352
7.3% CO_2	-4	633.49734	5.5% CO_2	-4	764.27286	3.6% CO_2	-4	957.7121
	-2	695.68146		-2	837.86636		-2	1048.142
29.1% C_2H_6	0	761.42929	21.8% C_2H_6	0	915.58957	14.6% C_2H_6	0	1143.575
	2	966.23542		2	1159.6393		2	1446.421
3.6% H_2S	4	1216.5085	2.7% H_2S	4	1456.8285	1.8% H_2S	4	1813.971
	6	1527.523		6	1826.363		6	2272.247
	8	1915.3887		8	2288.0317		8	2847.461
	10	2402.1208		10	2869.3316		10	3577.033

Table B12:Hydrate temperature and pressure formation for CH_4, CO_2, H_2S (WGR 1)

Composition	T(°C)	P(kPa)	Composition	T(°C)	P(kPa)
	-10	985.98134		-10	1901.5141
90% CH_4	-8	1086.9475	100% CH_4	-8	2049.6528
	-6	1194.5506		-6	2203.5946
1.8% CO_2	-4	1308.8348	0% CO_2	-4	2363.0599
	-2	1429.8015		-2	2527.7168
7.3% C_2H_6	0	1557.4013	0% C_2H_6	0	2697.1892
	2	1969.9693		2	3323.646
0.9% H_2S	4	2468.8747	0% H_2S	4	4041.3997
	6	3095.5069		6	4916.7678
	8	3890.7349		8	5991.5142
	10	4915.578		10	7322.6481

Table B13:Hydrate temperature and pressure formation for CH_4, CO_2, C_2H_6, H_2S (WGR 3)

Composition	T(°C)	P(kPa)	Composition	T(°C)	P(kPa)	Composition	T(°C)	P(kPa
	-10	470.87651		-10	571.22253		-10	719.468
60% CH_4	-8	522.63984	70% CH_4	-8	632.71183	80% CH_4	-8	795.177
	-6	578.05082		-6	698.42321		-6	875.968
7.3% CO_2	-4	637.12859	5.5% CO_2	-4	768.37608	3.6% CO_2	-4	961.868
	-2	699.86248		-2	842.5567		-2	1052.86
29.1% C_2H_6	0	766.20923	21.8% C_2H_6	0	920.9166	14.6% C_2H_6	0	1148.91
	2	973.4984		2	1167.6252		2	1454.31
3.6% H_2S	4	1227.2762	2.7% H_2S	4	1468.4883	1.8% H_2S	4	1825.32
	6	1543.3263		6	1843.2275		6	2288.42
	8	1938.4034		8	2312.2385		8	2870.34
	10	2435.4384		10	2903.8875		10	3609.25

Table B14:Hydrate temperature and pressure formation for CH_4, CO_2, H_2S (WGR 3)

Composition	T(°C)	P(kPa)	Composition	T(°C)	P(kPa)
	-10	988.86371		-10	1901.5141
90% CH_4	-8	1090.2362	100% CH_4	-8	2049.6528
	-6	1198.28		-6	2203.5946
1.8% CO_2	-4	1313.0444	0% CO_2	-4	2363.0599
	-2	1434.5279		-2	2527.7168
7.3% C_2H_6	0	1562.681	0% C_2H_6	0	2697.1892
	2	1977.5768		2	3323.646
0.9% H_2S	4	2479.4982	0% H_2S	4	4041.3997
	6	3110.242		6	4916.7678
	8	3911.0682		8	5991.5142
	10	4943.5205		10	7322.6481

Table B15:Hydrate temperature and pressure formation for CH_4, CO_2, C_2H_6, H_2S (WGR 7)

Composition	T(°C)	P(kPa)	Composition	T(°C)	P(kPa)	Composition	T(°C)	P(kPa)
	-10	475.47078		-10	576.36224		-10	725.024
60% CH_4	-8	528.04184	70% CH_4	-8	638.68352	80% CH_4	-8	801.549
	-6	584.35254		-6	705.31165		-6	883.230
7.3% CO_2	-4	644.42496	5.5% CO_2	-4	776.26646	3.6% CO_2	-4	970.094
	-2	708.24738		-2	851.53336		-2	1062.12
29.1% C_2H_6	0	775.77496	21.8% C_2H_6	0	931.06041	14.6% C_2H_6	0	1159.27
	2	987.94017		2	1182.6209		2	1469.30
3.6% H_2S	4	1248.5038	2.7% H_2S	4	1490.0567	1.8% H_2S	4	1846.37
	6	1574.1459		6	1873.8894		6	2317.68
	8	1982.6712		8	2355.3997		8	2910.68
	10	2498.4777		10	2964.1713		10	3664.49

Table B16:Hydrate temperature and pressure formation for CH_4, CO_2, H_2S (WGR 7)

Composition	T(°C)	P(kPa)	Composition	T(°C)	P(kPa)
	-10	993.56641		-10	1901.5141
90% CH_4	-8	1095.6158	100% CH_4	-8	2049.6528
	-6	1204.3968		-6	2203.5946
1.8% CO_2	-4	1319.9542	0% CO_2	-4	2363.0599
	-2	1442.2872		-2	2527.7168
7.3% C_2H_6	0	1571.3443	0% C_2H_6	0	2697.1892
	2	1989.9654		2	3323.646
0.9% H_2S	4	2496.5992	0% H_2S	4	4041.3997
	6	3133.6014		6	4916.7678
	8	3942.6954		8	5991.5142
	10	4986.0428		10	7322.6481

APPENDIX C

K-METHOD RESULTS

Table C1: Pressure for hydrate formation at 2°C for CH_4, CO_2 and H_2S (WGR 5.75)

Pressure (kPa)	Vapor Fraction y	Solid Fraction x	CH_4 vapor y/%	CO_2 vapor y/%	H_2S vapor y/%	CH_4 solid x/%	CO_2 solid x/%	H_2S solid x/%
1730.58	0.99	0.01	90.6%	5.5%	3.9%	50.4%	5.9%	43.7%
2282.16	0.89	0.11	93.3%	5.2%	1.5%	65.6%	7.7%	26.7%
2585.53	0.79	0.21	94.4%	4.8%	0.8%	74.5%	7.9%	17.6%
2744.11	0.69	0.31	95.1%	4.5%	0.4%	79.5%	7.7%	12.8%
2840.64	0.59	0.41	95.5%	4.1%	0.4%	82.6%	7.4%	10.0%
2902.69	0.49	0.51	95.9%	3.9%	0.2%	84.8%	7.0%	8.2%
2950.96	0.39	0.61	96.2%	3.6%	0.2%	86.5%	6.6%	6.9%
2985.43	0.29	0.71	96.4%	3.4%	0.2%	87.7%	6.3%	6.0%
3013.01	0.19	0.81	96.6%	3.2%	0.2%	88.7%	6.0%	5.3%
3033.69	0.09	0.91	96.4%	3.4%	0.2%	89.6%	5.7%	4.7%

Table C2: Pressure for hydrate formation at 6°C for CH_4, CO_2 and H_2S (WGR 5.75)

Temperature : 6°C								
Pressure (kPa)	Vapor Fraction y	Solid Fraction x	CH_4 vapor y/%	CO_2 vapor y/%	H_2S vapor y/%	CH_4 solid x/%	CO_2 solid x/%	H_2S solid x/%
2585.53	0.99	0.01	90.6%	5.4%	4.0%	56.6%	5.6%	37.8%
3268.11	0.89	0.11	92.9%	5.3%	1.8%	68.9%	7.0%	24.1%
3668.01	0.79	0.21	94.0%	4.9%	1.1%	76.1%	7.4%	16.5%
3902.43	0.69	0.31	94.6%	4.6%	0.8%	80.5%	7.3%	12.2%
4047.22	0.59	0.41	95.1%	4.3%	0.6%	83.2%	7.1%	9.7%
4143.75	0.49	0.51	95.5%	4.1%	0.4%	85.2%	6.8%	8.0%
4219.59	0.39	0.61	95.8%	3.8%	0.4%	86.7%	6.5%	6.8%
4274.75	0.29	0.71	96.1%	3.6%	0.3%	87.8%	6.2%	6.0%
4323.01	0.19	0.81	96.3%	3.4%	0.3%	88.8%	5.9%	5.3%
4257.49	0.09	0.91	96.5%	3.3%	0.2%	89.6%	5.7%	4.7%

Table C3: Pressure for hydrate formation at 10°C for CH_4, CO_2 and H_2S (WGR 5.75)

Temperature : 10°C								
Pressure (kPa)	Vapor Fraction y	Solid Fraction x	CH_4 vapor y/%	CO_2 vapor y/%	H_2S vapor y/%	CH_4 solid x/%	CO_2 solid x/%	H_2S solid x/%
3895.54	0.99	0.01	90.5%	5.5%	4.0%	64.1%	4.8%	31.1%
4681.54	0.89	0.11	92.3%	5.4%	2.3%	73.2%	5.9%	20.9%
5171.07	0.79	0.21	93.3%	5.2%	1.5%	78.6%	6.4%	15.0%
5467.54	0.69	0.31	94.5%	4.7%	0.8%	84.1%	6.5%	9.4%
5674.39	0.59	0.41	94.5%	4.7%	0.8%	84.1%	6.5%	9.4%
5826.07	0.49	0.51	94.8%	4.5%	0.7%	85.8%	6.4%	7.8%
5929.49	0.39	0.61	95.2%	4.3%	0.5%	87.1%	6.2%	6.7%
5998.44	0.29	0.71	95.6%	4.1%	0.3%	88.0%	6.0%	6.0%
6094.97	0.19	0.81	95.7%	3.9%	0.4%	89.0%	5.8%	5.2%
6150.12	0.09	0.91	95.9%	3.7%	0.4%	89.7%	5.6%	4.7%

Table C4: Pressure for hydrate formation at 2°C for CH_4, CO_2, C_2H_6 and H_2S (WGR 5.75)

Temperature : 2°C										
Pressure (kPa)	Vapor Fraction y	Solid Fraction x	CH_4 vapor y/%	CO_2 vapor y/%	C2H6 vapor y/%	H_2S vapor y/%	CH_4 solid x/%	CO_2 solid x/%	C_2H_6 solid x/%	H_2S solid x/%
1585.79	0.99	0.01	89.4%	1.5%	8.3%	0.8%	46.6%	1.5%	42.7%	9.2%
1854.69	0.89	0.11	93.2%	1.4%	5.0%	0.4%	54.8%	1.7%	38.0%	5.5%
2151.16	0.79	0.21	95.7%	1.4%	2.7%	0.2%	66.2%	2.0%	31.6%	0.2%
2392.48	0.69	0.31	97.0%	1.3%	1.5%	0.2%	71.1%	1.9%	24.0%	3.0%
2564.85	0.59	0.41	97.7%	1.1%	1.1%	0.1%	76.5%	1.9%	19.3%	2.3%
2682.06	0.49	0.51	98.1%	1.0%	0.8%	0.1%	80.2%	1.9%	16.1%	1.8%
2771.69	0.39	0.61	98.3%	1.0%	0.6%	0.1%	83.0%	1.8%	13.7%	1.5%
2833.75	0.29	0.71	98.5%	1.0%	0.5%	0.0%	85.1%	1.7%	11.9%	1.3%
2882.01	0.19	0.81	98.7%	0.9%	0.4%	0.0%	86.7%	1.6%	10.5%	1.2%
2923.38	0.09	0.91	98.8%	0.9%	0.3%	0.0%	88.0%	1.6%	9.4%	1.0%

Table C5: Pressure for hydrate formation at 6°C for CH_4, CO_2, C_2H_6 and H_2S (WGR 5.75)

Temperature : 6°C										
Pressure (kPa)	Vapor Fraction y	Solid Fraction x	CH_4 vapor y/%	CO_2 vapor y/%	C2H6 vapor y/%	H_2S vapor y/%	CH_4 solid x/%	CO_2 solid x/%	C_2H_6 solid x/%	H_2S solid y/%
2489.01	0.99	0.01	89.3%	1.5%	8.3%	0.9%	54.4%	1.5%	35.8%	8.3%
2833.75	0.89	0.11	92.4%	1.5%	5.7%	0.4%	61.7%	1.7%	31.5%	5.1%
3164.69	0.79	0.21	94.4%	1.4%	3.9%	0.3%	68.4%	1.8%	26.2%	3.6%
3440.48	0.69	0.31	95.8%	1.3%	2.7%	0.2%	73.9%	1.9%	21.6%	2.6%
3654.22	0.59	0.41	96.6%	1.2%	2.1%	0.1%	78.1%	1.8%	18.0%	2.1%
3819.7	0.49	0.51	97.1%	1.2%	1.6%	0.1%	81.2%	1.8%	15.3%	1.7%
3930.01	0.39	0.61	97.6%	1.1%	1.3%	0.0%	83.5%	1.7%	13.2%	1.6%
4026.54	0.29	0.71	97.9%	1.0%	1.1%	0.0%	85.4%	1.7%	11.6%	1.3%
4109.28	0.19	0.81	98.2%	0.9%	0.9%	0.0%	86.9%	1.6%	10.4%	1.1%
4164.43	0.09	0.91	98.4%	0.9%	0.7%	0.0%	88.1%	1.6%	9.4%	0.9%

Table C6: Pressure for hydrate formation at 10°C for CH_4, CO_2, C_2H_6 and H_2S (WGR 5.75)

Temperature : 10°C										
Pressure (kPa)	Vapor Fraction y	Solid Fraction x	CH_4 vapor y/%	CO_2 vapor y/%	C2H6 vapor y/%	H_2S vapor y/%	CH_4 solid x/%	CO_2 solid x/%	C_2H_6 solid x/%	H_2S solid y/%
3964.49	0.99	0.01	89.3%	1.5%	8.4%	0.8%	63.9%	1.3%	27.5%	7.3%
4350.59	0.89	0.11	91.4%	1.5%	6.6%	0.5%	69.3%	1.5%	24.6%	4.6%
4757.58	0.79	0.21	93.0%	1.4%	5.2%	0.4%	73.8%	1.6%	21.4%	3.2%
4957.33	0.69	0.31	94.2%	1.4%	4.2%	0.2%	77.3%	1.7%	18.4%	2.6%
5184.86	0.59	0.41	95.1%	1.3%	3.4%	0.2%	80.2%	1.7%	16.0%	2.1%
5377.91	0.49	0.51	95.7%	1.3%	2.8%	0.2%	82.5%	1.7%	14.0%	1.8%
5522.7	0.39	0.61	96.3%	1.2%	2.4%	0.1%	84.4%	1.6%	12.4%	1.6%
5653.7	0.29	0.71	96.6%	1.2%	2.1%	0.1%	85.9%	1.6%	11.2%	1.3%
5757.12	0.19	0.81	97.0%	1.0%	1.9%	0.1%	87.1%	1.6%	10.2%	1.1%
5860.84	0.09	0.91	97.2%	1.0%	1.8%	0.0%	88.2%	1.5%	9.3%	1.0%

APPENDIX D

KEY MILESTONE

First Semester (July 2008- December 2009)

No.	Detail/ Week	1	2	3	4	5	6	7	8	9	10		11	12	13	14
1	Selection of Project Topic	▨	▨									Mid-semester break				
2	Preliminary Research Work		▨	▨	▨											
3	Submission of Preliminary Report															
4	Seminar 1 (optional)					▨	▨	▨								
5	Project Work					▨	▨	▨	▨	▨	▨					
6	Submission of Progress Report															
7	Seminar 2 (compulsory)												▨	▨	▨	
8	Project work continues												▨	▨	▨	
9	Submission of Interim Report Final Draft														▨	
10	Oral Presentation															▨

Second Semester (January 2009-June 2009)

No.	Detail/ Week	1	2	3	4	5	6	7	8	9		10	11	12	13	14	15
1	Continuation on Project	▨	▨	▨							Mid-semester break						
2	Submission of Progress Report			▨													
3	Simulation continues				▨	▨	▨	▨	▨	▨		▨					
4	Submission of Final Report (Draft)												▨				
5	Pre-Edx / Seminar													▨			
6	Final Oral Presentation																
7	Submission of Final Hardbound																▨